Primljen / Received: 15.11.2025.
Ispravljen / Corrected: 5.12.2025.
Prihvaćen / Accepted: 8.12.2025.
Dostupno online / Available online: 15.12.2025.

Liquefaction in Croatia: Risk assessment and rapid post-earthquake decision-making – five years later

Authors:

Prof. **Meho Saša Kovačević**, PhD. CE
University of Zagreb
Faculty of Civil Engineering
meho.sasa.kovacevic@grad.unizg.hr
Corresponding author

Assoc.Prof. **Mario Bačić**, PhD. CE
University of Zagreb
Faculty of Civil Engineering
mario.bacic@grad.unizg.hr

Assist.Prof. **Lovorka Librić**, PhD. CE
University of Zagreb
Faculty of Civil Engineering
lovorka.libric@grad.unizg.hr

Prof. **Danijela Jurić-Kaćunić**, PhD. CE
University of Zagreb
Faculty of Civil Engineering
danijela.juric.kacunic@grad.unizg.hr

Original research paper

Meho Saša Kovačević, Mario Bačić, Lovorka Librić, Danijela Jurić Kaćunić

Liquefaction in Croatia: Risk assessment and rapid post-earthquake decision-making – five years later

After the 2020 Petrinja earthquake, the area of Sisak-Moslavina County became the focus of intensive scientific research and professional activities related to liquefaction. This paper provides an overview of the documentation and quantification of liquefaction occurrences over a five-year period, including field observations, the development of preliminary susceptibility maps, and the application of various in-situ and laboratory methods to assess soil resistance. Particular emphasis is placed on the use of different geotechnical investigation methods to evaluate cyclic soil resistance and identify areas with increased liquefaction risk, which enabled rapid decision-making in post-earthquake recovery and infrastructure rehabilitation. The study highlights the importance of combining preliminary assessments with detailed geotechnical investigations to support post-earthquake reconstruction. Additionally, recommendations are provided for future activities, including detailed liquefaction microzonation for Sisak-Moslavina County, the definition of guidelines for future investigation work within specific projects, especially those related to linear infrastructure, where soil variability is highly pronounced, and the integration of investigated locations into international databases to contribute to the global calibration of liquefaction assessment charts.

Key words:
Petrinja earthquake, liquefaction, geotechnical investigations, post-earthquake reconstruction

Izvorni znanstveni rad

Meho Saša Kovačević, Mario Bačić, Lovorka Librić, Danijela Jurić Kaćunić

Likvefakcija u Hrvatskoj: procjena rizika i brze postpotresne odluke – pet godina poslije

Nakon petrinjskog potresa iz 2020. godine, područje Sisačko-moslavačke županije postalo je središte intenzivnih znanstvenoistraživačkih i stručnih aktivnosti vezanih uz likvefakciju. Rad daje pregled evidentiranja i kvantifikacije pojave likvefakcije u razdoblju od pet godina, uključujući terenska opažanja, izradu preliminarnih karata podložnosti te primjenu različitih in-situ i laboratorijskih metoda za procjenu otpornosti tla. Poseban naglasak stavljen je na primjenu različitih geotehničkih metoda ispitivanja tla za procjenu cikličkog otpora tla i identifikaciju područja s povećanim rizikom od likvefakcije, što je omogućilo brzo donošenje odluka u postpotresnoj obnovi i sanaciji infrastrukture. Rad ističe važnost kombiniranja preliminarnih procjena s detaljnim geotehničkim istraživanjima za podršku postpotresnoj obnovi. Dodatno, dane su preporuke za buduće aktivnosti, uključujući detaljnu mikrozonaciju likvefakcijskog potencijala za područje Sisačko-moslavačke županije, definiranje smjernica za buduće istražne radove u sklopu konkretnih projekata, osobito onih koji se odnose na linijsku infrastrukturu gdje je varijabilnost tla izrazito naglašena te uvrštavanje istraženih lokacija u međunarodne baze podataka radi doprinosa globalnoj kalibraciji dijagrama za procjenu likvefakcije.

Ključne riječi:
petrinjski potres, likvefakcija, geotehnička istraživanja, postpotresna obnova

1. Introduction

Over the past century, earthquakes in Europe have caused immense human and material losses, with estimates exceeding 200,000 fatalities and reaching hundreds of billions of euros in damage [1]. While seismic risk is most often associated with the performance and resilience of buildings and infrastructure, evidence from a number of recent earthquakes shows that soil-related phenomena, among which liquefaction is the most prominent, can be equally, or even more, destructive. Numerous studies indicate that a substantial share of total economic losses can be attributed to liquefaction effects, particularly in areas characterized by a high groundwater table and widespread alluvial sediments [2].

Liquefaction is a geotechnical process in which saturated, loose sands and silty sands lose part of, or nearly all of, their shear strength during strong earthquake shaking [3]. Over a short period of time, such layers behave like a viscous fluid and temporarily cease to function as a load-bearing medium. The consequences include exceedance of serviceability and ultimate limit states of both underground and surface infrastructure. Despite advances in experimental, numerical, and field investigations, liquefaction remains one of the most challenging earthquake-induced mechanisms due to its pronounced spatial variability and the suddenness of its occurrence. The scientific community therefore continues to intensify efforts to improve understanding of soil response under dynamic loading, while also developing and refining appropriate mitigation measures [4]. It should be emphasized that soil that has liquefied once has not necessarily gained sufficient resistance to liquefaction. Re-liquefaction may occur during subsequent seismic events. Moreover, numerous studies [5–8] indicate that a prior liquefaction episode does not necessarily make the soil more resistant, and re-liquefaction during later earthquakes is not uncommon.

Systematic research on liquefaction developed in the aftermath of the 1964 Niigata earthquake [9], which provided some of the first detailed documentation of the phenomenon and catalysed the development of the empirical procedures and engineering criteria that underpin modern practice. Since then, theoretical understanding and mitigation approaches have advanced considerably. However, liquefaction occurrence still depends strongly on local soil conditions, the geological setting, and the intensity of seismic excitation. Although liquefaction in Croatia was only rarely discussed in modern scientific and professional literature until 2020, historical records indicate that the phenomenon occurred earlier as well, particularly within the Pannonian Basin. Overviews of these events are provided by Veinović [10] and Mijić et al. [11]. Liquefaction manifestations were reported during the 1757 Virovitica earthquake, the 1880 Zagreb earthquake, and the 1909 Pokupsko earthquake, and even during earthquakes affecting the wider Dubrovnik region (notably the 1667 and 1979 events). In continental Croatia, liquefaction was predominantly observed in alluvial plains along the major rivers, the Drava, Sava, and Kupa, where loose, water-saturated sediments favourable for liquefaction are widespread. For the 1757 Virovitica earthquake, chronicles describe ground cracking and the eruption of water mixed with yellow sand at multiple locations, including the infilling of deep wells with sediment. During the 1880 Zagreb earthquake, whose magnitude was substantially larger than that of the 2020 Zagreb event, several sites reported the expulsion of greyish sand from fissures and the formation of conical sand accumulations, occasionally of impressive size [12]. Similar manifestations were documented after the 1909 Pokupsko earthquake, where fissuring along the Kupa River again highlighted the susceptibility of shallow alluvial deposits to dynamic loading. Collectively, these historical accounts confirm that Croatian alluvial deposits have repeatedly exhibited a propensity for liquefaction, providing valuable context for interpreting contemporary events.

In contrast to the historically documented but spatially limited occurrences, the liquefaction recorded after the 2020 Mw 6.4 earthquake with an epicentre near Petrinja represents the largest confirmed large-scale liquefaction event in Croatia to date. In a paper published immediately after the Zagreb earthquake [3], in which liquefaction was not observed primarily due to the relatively low earthquake magnitude, the authors presented the key aspects addressed by geotechnical earthquake engineering. Shortly thereafter, the Petrinja earthquake occurred. The intensity of ground shaking, an elevated groundwater table, and extensive alluvial deposits in the valleys of the Kupa, Sava, Glina, and Maja rivers created favourable conditions for liquefaction over an estimated area of approximately 600 km², within a radius of roughly 20 km from the epicentre. A detailed inventory of liquefaction locations, identified from aerial imagery and documented by field teams, was provided by Mijić et al. [11], as shown in Figure 1.

Liquefaction manifestations in Sisak–Moslavina County were spatially very distinct, primarily as a series of linearly aligned sand ejecta features that followed straight ground-surface fissures. The broader area of the county is underlain by Neogene and Quaternary deposits. The Neogene succession comprises coarse- and fine-grained clastics, conglomerates, gravels and sands, as well as marls, clays and sandstones (M_2). The Badenian (M_4) and Sarmatian (M_5) deposits are of similar composition. The Pannonian (M_6) deposits are represented by limestones and marls, overlain by Pontian (M_7) sediments (marls and claystones with sands). However, the highest concentration of liquefaction occurrences was recorded along the Sava, Kupa and Glina rivers, where the recent alluvium contains predominantly clean sands, locally silty or gravelly sands, and occasional lenses of coarser gravel [13]. The alluvial sediments consist mainly of sands, locally mixed with silty and clayey fractions, and display variable mineralogical composition, including quartz, rock fragments, and occasional carbonates. Floodplain deposits are predominantly clayey and sandy silts, formed by the deposition of fine-grained material during flooding events. These sediments reflect the dynamic depositional environment of the rivers and their floodplains, with local sediment thicknesses reaching several metres. At the ground surface, liquefaction processes manifested through a range of geomorphic features and infrastructure damage: from extensive fissure zones (Figure 2a),

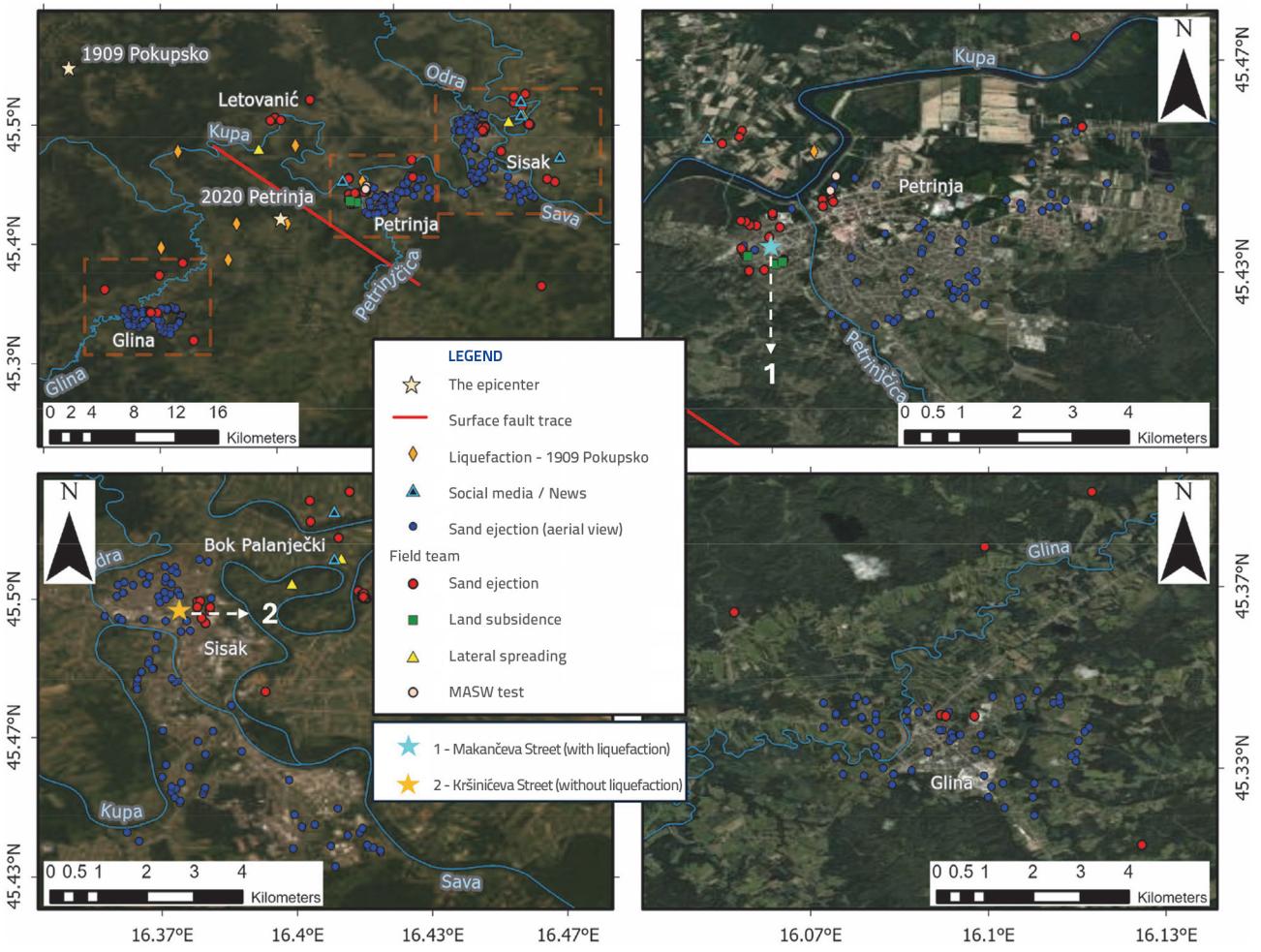

Figure 1. Satellite map of the Petrinja, Sisak, and Glina area with the locations of documented liquefaction manifestations during the 2020 Petrinja earthquake; adapted from Mijić et al. [11], with the locations (1 and 2) indicated where the liquefaction potential analysis is conducted in this study

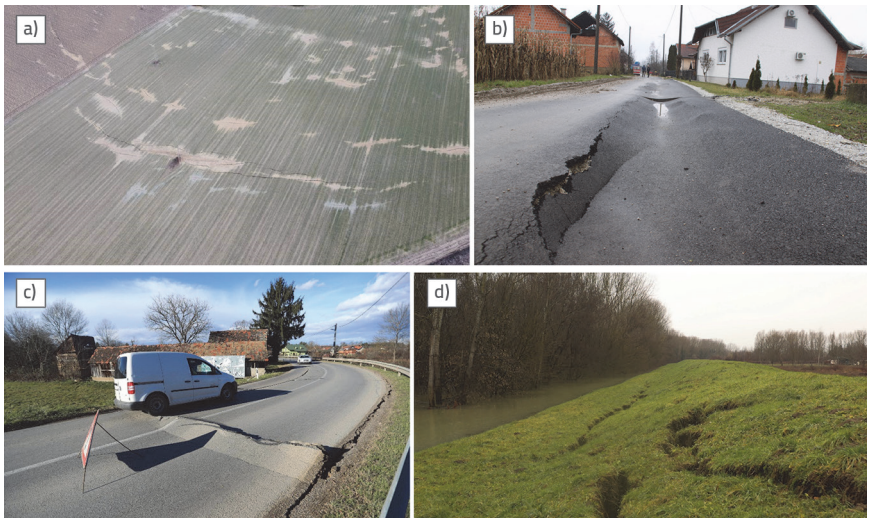

Figure 2. Liquefaction manifestations associated with foundation soils and infrastructure during the 2020 Petrinja earthquake: (a) longitudinal fissures with sand ejecta, (b), (c) deformed roadways (c—photo: Slavko Midzor/Edina Zuko/PIXSELL), (d) cracks in a levee (photo: Tomislav Novosel / Croatian Waters)

through settlements and deformations of transport infrastructure (Figures 2b and 2c), to severe damage to levees (Figure 2d), where cracking and lateral displacement were observed as a consequence of the loss of bearing capacity in the foundation soils. Deformations and failures were also recorded in other linear infrastructure systems, such as water-supply and sewer networks. In addition, issues were identified at bridges and their abutments, where partial soil destabilisation led to movements and deformations of the bridge structure and temporary traffic restrictions.

The above geotechnical problems that occurred during and after the Petrinja earthquake provide the basis for the more detailed discussion that follows.

The aim of this paper is to provide a concise yet comprehensive overview of the key findings, activities, and procedures developed and applied in the five years following the Petrinja earthquake, with a particular focus on understanding and managing liquefaction risk. The first part reviews the most important scientific, research, and professional activities carried out in Sisak–Moslavina County, including the preparation of a liquefaction inventory and the collection of data required for subsequent analyses. This is followed by a presentation of the approaches used to assess liquefaction potential under the conditions of accelerated post-earthquake reconstruction, highlighting the reasons why certain procedures, most notably the cyclic stress method, have become dominant in domestic practice. The methodology is then demonstrated at two representative sites, one that experienced liquefaction and one that did not, with the aim of emphasizing differences in the properties of the alluvial deposits and illustrating the practical application of the procedure under real-world, field-based decision-making constraints. Finally, the paper provides a brief overview of ground-improvement technologies implemented during the reconstruction process and offers recommendations for further improving assessment frameworks and procedures, with particular emphasis on the importance of systematic data collection and the integration of multiple investigation methods.

2. Scientific, research and professional activities in Sisak–Moslavina County

Following the 2020 Petrinja earthquake, Sisak–Moslavina County became the focus of exceptionally intensive scientific and professional efforts aimed at documenting, understanding, and quantifying liquefaction occurrence. In the first months after the event, the emphasis was on systematic mapping of surface manifestations and preliminary assessments of the spatial extent of the phenomenon, while subsequent investigations involved advanced geotechnical and geophysical testing to characterise soil properties and evaluate resistance to cyclic loading.

One of the key early, and highly valuable, initiatives was the development of preliminary liquefaction susceptibility maps for the broader earthquake-affected area [14]. For this purpose, a heuristic approach was adopted, based on well-established preconditions for liquefaction: the presence of loose granular layers below the groundwater table, a high groundwater level, seismic excitation with peak ground acceleration $a_g \geq 0.10$ g, and the locations where liquefaction was documented during the Petrinja earthquake. To support this effort, a map of surface liquefaction manifestations was compiled based on field reconnaissance, including sand boils at the ground surface, infilling of wells with sand and/or sand ejection from wells, and sand ejection along building foundations both inside and outside structures. Over larger areas, photogrammetric surveys were performed using an unmanned aerial vehicle. The input data for the methodology comprised:

1. the above preliminary liquefaction inventory,
2. the geological setting, where stratigraphic units of Holocene alluvial deposits were adopted from the Basic Geological Map (OGK),
3. topography derived from a digital elevation model,
4. the locations of watercourses and oxbow channels digitised from topographic maps and satellite imagery.

Data availability largely governed the spatial resolution and reliability of the final model. The results of the methodology, shown in Figure 3, were synthesised into a preliminary liquefaction susceptibility map. However, the authors emphasise that this is an initial assessment, since key geotechnical parameters, such as the thickness of the non-liquefiable overburden, the geotechnical properties of potentially liquefiable layers, and detailed groundwater-level maps, were not available at that time. The need for systematic and detailed geotechnical investigations is therefore highlighted, as only precise information on geological structure, geotechnical characteristics of the deposits, and groundwater conditions will enable the production of high-resolution susceptibility maps tailored to the needs of local communities and spatial-planning documents. An important component consists of special conditions for reconstruction or new construction, which, across all susceptibility levels, from low to high, emphasise the mandatory implementation of geotechnical investigations that include an assessment of liquefaction potential. The resulting map was integrated into the interactive ISPU portal [15] of the Ministry of Construction, Physical Planning and State Assets.

An additional contribution to the early reconnaissance efforts was provided in the GEER report [16], which presents selected earthquake-induced manifestations, including liquefaction on agricultural, sports, and other open areas, in most cases located in close proximity to watercourses. The sites were mapped based on field observations, reports from local collaborators, and notifications from residents. These early overview studies played an important role in establishing an initial understanding of the spatial distribution of liquefaction, while also identifying priority locations for the detailed geotechnical and geophysical investigations that followed. One of the first studies to provide an inventory of the resulting surface deformations was that of Pollak et al. [17], in which the authors collected and systematised a large set of input data and developed a preliminary

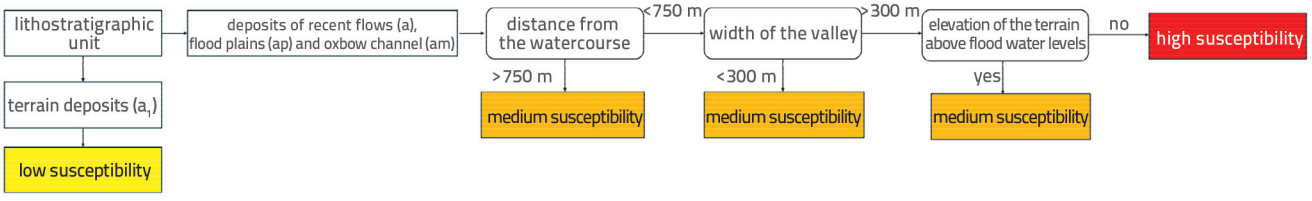

Figure 3. Methodology for developing the preliminary liquefaction susceptibility map for Sisak–Moslavina County, adapted from [14]

database of critical zones of damage and ground deformation. At the time of publication, the database included 85 locations with liquefaction manifestations. An analysis of the distances between sand-ejection features (i.e. boiling sand) and the Kupa, Sava, and Glina rivers indicated a strong link between liquefaction occurrence and alluvial deposits, with distances typically within 1 km of the river channels. As a preliminary conclusion, the authors noted that liquefaction manifestations were almost exclusively recorded within extensive alluvial sediments characterised by pronounced layers of loose sand. During a similar period, Tondi et al. [18] published a study focused on a comprehensive description of primary and secondary earthquake effects. Although liquefaction was not the central topic, the authors documented a number of liquefaction-induced fissures and other secondary geomorphic effects. A third important early study is the reconnaissance paper by Baize et al. [19], in which a European interdisciplinary team of geologists and engineers mapped more than 700 distinct deformation features, including fissures, fault zones, landslides, and liquefaction-related phenomena, based on three field campaigns conducted in early 2021. Liquefaction manifestations were documented through a combination of field mapping and remote sensing, resulting in approximately 200 phenomenological records across an area of about 600 km² between the river valleys of the Kupa, Glina, and Sava. The authors note that the preliminary findings are broadly consistent with existing empirical relationships for liquefaction distance and intensity [20–22], while the large volume of newly collected data offers substantial potential to refine these methods and to develop more accurate site-scale criteria. The most recent and most comprehensive account of liquefaction inventory development is provided by Amoroso et al. [23], who analyse a total of 61 sites in the Petrinja area by combining field observations with laboratory testing for soil classification and determination of sediment composition. The adopted workflow enabled a detailed geological and geotechnical characterisation of all locations where liquefaction was observed. Data collected during post-earthquake field surveys, together with sedimentological and geotechnical analyses, were systematically organised into standardised site forms, thereby creating a valuable resource for subsequent seismological, geological, and geotechnical research.

All of the above studies represent foundational efforts in establishing preliminary databases and liquefaction inventories for Sisak–Moslavina County, relying on extensive field observations, remote sensing, and broad spatial coverage. In doing so, they provided the initial framework for understanding the regional-scale spatial distribution of liquefaction manifestations across the affected area. In parallel, numerous investigations have focused on targeted geotechnical and/or geophysical studies at individual sites. These studies apply a range of in-situ and laboratory methods, often in combination, to obtain a more detailed insight into the local stratigraphic, geotechnical, and seismological characteristics of the ground. Although site-specific in scope, their results are highly important, as they complement the regional datasets and enable their validation, calibration, and future refinement.

The first study in this series is Bačić et al. [24], which analyses liquefaction potential as a cause of roadway deformation and settlement at the Nova Drenčina site. A comparison of CPT and MASW results at four locations showed that, despite local discrepancies between the datasets, the liquefaction factors of safety derived using the two methods exhibit relatively consistent trends. The study highlights the importance of combining different ground investigation methods when assessing liquefaction potential. Building on this work, Bačić et al. [25] focused on a levee near the Krnjica settlement, which suffered substantial damage due to liquefaction. The authors developed a methodology for generating synthetic CPT profiles from measured shear-wave velocities, enabling liquefaction assessment even at locations where CPT soundings were not performed. Although the synthetic approach generally underestimated the CPT tip resistance (q_c), the resulting factors of safety and the spatial distribution of potentially liquefiable zones agreed well with the outcomes obtained from the available CPT data. A further study by the same research group [26] focused on the levee at Galdovo, where three in-situ methods were applied to investigate the foundation soils: CPT, SPT, and MASW. A comparison of cyclic resistance estimates indicated that the CPT-based approach yields higher liquefaction probabilities, whereas the SPT- and i v_s-based methods generally produce lower results that are mutually comparable. The authors emphasise that a comprehensive spatial assessment requires explicit consideration of both vertical and horizontal soil heterogeneity, which is the focus of their ongoing work.

In addition to Croatian research teams, substantial contributions were also made by authors from international research consortia. Amoroso et al. [27] carried out an integrated geological–geotechnical and geophysical campaign at ten sites along the Kupa, Glina, and Sava rivers. The programme included in-situ testing such as dynamic DPT probing and Medusa DMT dilatometer tests, combined with extensive geophysical profiling, providing detailed insights into the properties of both liquefied and non-liquefied strata. Subsequently, Moiriat et al. [28] focused on the structural characterisation and mechanical properties of alluvial deposits along the Kupa River. Their investigation employed dynamic CPT soundings (DCPT), light (DPL) and heavy (DPSH) dynamic probing, as well as electrical resistivity tomography (ERT) and ground-penetrating radar (GPR). Borehole core samples were also collected for calibration purposes. The authors presented preliminary interpretations of the dataset and highlighted the potential of integrated methods for accurately identifying layers susceptible to liquefaction.

In addition to the extensive scientific and research activities, a crucial component of the post-earthquake period comprised geotechnical and geophysical investigations carried out to support the reconstruction of existing structures and the construction of new residential and infrastructure facilities. Particularly noteworthy was a large-scale, purpose-designed investigation campaign involving boreholes, CPT testing, and multiple geophysical methods to achieve a detailed characterisation of the geotechnical–geological conditions beneath a series of levees. These levees experienced significant deformations and local failures during the earthquake, and the investigation results provide the basis for their rehabilitation [29, 30].

The most extensive professional engagement of the geotechnical community, however, was associated with the preparation of geotechnical reports for replacement houses and buildings within the post-earthquake reconstruction programme led by the Ministry

of Physical Planning, Construction and State Assets. Given the large number of sites and the need for rapid yet reliable engineering judgement, a standardised methodology was established based on a combination of CPT testing and the SASW geophysical method. This approach enabled sufficiently fast and accurate estimation of key parameters: foundation bearing capacity, soil type in terms of local amplification effects, a preliminary assessment of site susceptibility to liquefaction, and the need for additional investigations at locations potentially affected by slope instability. To date, approximately 400 sites have been investigated using this methodology, representing the largest systematically collected dataset on geotechnical soil properties in Sisak–Moslavina County to date. Beyond its immediate application in reconstruction, this dataset will have lasting value and can serve as a robust basis for future initiatives aimed at comprehensive liquefaction potential assessment and more detailed county-scale microzonation analyses.

3. Approaches to liquefaction potential assessment under post-earthquake reconstruction conditions

In practice, a wide range of methods is available for assessing the liquefaction potential of soils. Laboratory testing provides detailed insight into the cyclic undrained response of geomaterials and yields highly valuable data for effective-stress analyses and the development of advanced numerical models. Cyclic densification and pore-pressure build-up are determined experimentally in drained and undrained cyclic tests with either controlled shear strain or controlled shear stress, most commonly expressed as the ratio of cyclic shear stress to mean effective stress. However, laboratory-based approaches involve several practical limitations, most notably the difficulty of obtaining high-quality undisturbed specimens. In addition, laboratory testing requires substantial time for sample preparation and execution, which constituted a limiting factor in the context of post-earthquake reconstruction. For these reasons, research in Sisak–Moslavina County over the past five years has shifted strongly toward in-situ investigation methods, in line with international trends that increasingly rely on field testing for liquefaction evaluation. Field tests such as the cone penetration test (CPT), the standard penetration test (SPT), and geophysical methods for determining shear-wave velocity have proven particularly suitable due to their reliability, accessibility, and routine use in Croatian engineering practice. Perhaps most importantly, the large number of sites required a rapid, reliable, and operational assessment of liquefaction potential in order to support decisions on remediation and ground treatment as part of the post-earthquake reconstruction process. Under these conditions, the simplified Cyclic Stress Approach (CSA) [31], together with empirical liquefaction triggering charts that are periodically updated in practice [32, 33], emerged as the key solution. These methods enable relatively fast estimation of factors of safety and the probability of liquefaction using standard in-situ data, making them well suited to urgent engineering interventions. The following sections provide an overview of the approach, the procedure for determining input and output parameters, and an analysis of results for two representative sites in the Petrinja area: one where liquefaction was documented and one where liquefaction did not occur.

3.1. Cyclic stress approach

The simplified stress-based procedure is often referred to as the "simplified method" and is the most widely used approach in practical geotechnical engineering for evaluating liquefaction triggering. The analysis requires the calculation or estimation of two key variables: the cyclic stress ratio (CSR), representing the seismic demand induced by the earthquake, and the cyclic resistance ratio (CRR), representing the soil's capacity to resist liquefaction.

To characterise the loading (CSR), the intensity of seismic action is quantified through the ratio between the induced shear stress and the effective vertical stress:

$$CSR = \frac{\tau_c}{\sigma'_{v0}} \tag{1}$$

Whereas in laboratory testing the cyclic shear stress amplitude τ_c is kept constant, in the field it varies throughout the shaking record. Therefore, the irregular shear-stress time history is commonly represented by an equivalent loading composed of a finite number of cycles at a constant shear-stress amplitude:

$$\tau_c = 0{,}65 \cdot \tau_{max} \tag{2}$$

The maximum shear stress in a soil layer, τ_{max} at the ground surface (surface layer of thickness *"h"*) may be estimated by assuming that the soil column behaves as a rigid block during earthquake shaking:

$$\tau_{max} = \frac{a_{max}}{g} \cdot \sigma_{v0} \tag{3}$$

Because the maximum shear stress decreases with depth (i.e., the soil column below the surface layer of thickness *"h"* does not behave as a rigid block), the expression is multiplied by the stress-reduction factor r_d, yielding the final form:

$$CSR = 0{,}65 \cdot \frac{a_{max}}{g} \cdot \frac{\sigma_{v0}}{\sigma'_{v0}} \cdot r_d \tag{4}$$

To characterise the soil resistance (CRR), it is necessary to quantify the resistance of the soil against loss of shear strength, i.e., liquefaction triggering. The resistance can be determined from laboratory testing or, more commonly in practice, estimated from in-situ tests. The parameter CRR represents the value of CSR required to trigger liquefaction. Liquefaction is triggered when:

$$CSR \geq CRR \tag{5}$$

The ratio of CRR to CSR defines the factor of safety:

$$FS = \frac{CRR}{CSR} \quad (6)$$

where a factor of safety of FS=1 denotes a state of *marginal stability*, values of FS < 1 indicate liquefaction triggering, whereas values of FS > 1 imply that the soil still has sufficient resistance and liquefaction is not expected to occur.

3.1.1. Determination of a representative peak ground acceleration for CSR calculation

For the purpose of defining the input value of the peak horizontal ground acceleration (a_{max}) in Eq. (4), design practice commonly follows the recommendations of EN 1998-1 [34] and the associated maps of design horizontal peak ground acceleration for ground type A for return periods T_p = 95 and 475 years, produced by the Department of Geophysics, Faculty of Science, University of Zagreb, and incorporated in the Croatian National Annex [35]. When determining the peak ground acceleration at the ground surface, the soil type at the site must also be considered. The influence of local ground conditions on seismic amplification is addressed in the aforementioned standard, for which Bačić et al. [3] provide a critical discussion.

Peak horizontal ground accelerations are primarily calibrated for shorter return periods, i.e., for the usual design levels of seismic action. However, the 2020 Petrinja earthquake produced peak horizontal ground accelerations that were significantly higher than those indicated by the hazard maps referenced in the standard. The most commonly used source for estimating horizontal ground acceleration for the Petrinja event is the USGS ShakeMap system [36]. Such a discrepancy is expected, because ShakeMap depicts the effects of an actual earthquake (instrumental recordings, macroseismic observations, and numerical interpolation), whereas the code hazard maps represent the long-term probability of exceedance. In other words, peak horizontal ground accelerations derived from ShakeMap do not necessarily match the values from the code maps, since the two represent conceptually different descriptions of seismic action. Given that previous liquefaction potential studies for the Petrinja area have predominantly adopted peak ground acceleration derived using the USGS methodology as the relevant input, the following section summarises this approach. The USGS estimate of peak horizontal ground acceleration is based on three main components: Modified Mercalli Intensity (MMI), "Did You Feel It?" macroseismic observations (DYFI), and empirical ground-motion prediction equations (GMPEs). This combined framework enables the construction of a spatial distribution of surface ground acceleration and provides a suitable input for CSR evaluation.

3.1.1.1. Modified mercalli intensity (MMI)

Modified Mercalli Intensity (MMI) is a descriptive earthquake intensity scale that ranks observed effects on people, buildings, and the natural environment using Roman numerals I–XII, from imperceptible to devastating. Unlike magnitude, the scale has no strict "mathematical" definition. Instead, it represents a systematic synthesis of macroseismic effects recorded at a given location. Although MMI is qualitative, decades of empirical research have established quantitative relationships between MMI and instrumental measures of ground motion, in particular peak horizontal ground acceleration (a_{max}, more commonly denoted as PGA) and peak ground velocity (PGV). Wald et al. [37] compared observed intensities with measured peak values for a series of California earthquakes and derived log–linear relationships. For the relevant intensity range, the authors report, for example, the following relation for PGA (V ≤ *I* ≤ VIII):

$$I = 3{,}66\log_{10} PGA - 1{,}66 \quad (7)$$

These relationships allow the expected PGA to be estimated from a given intensity level *I*:

$$PGA = 10^{\frac{I+1{,}66}{3.66}} \quad (8)$$

MMI increases approximately linearly with the logarithm of PGA, such that an increase in intensity by about one unit typically implies a multiple increase in PGA, although the exact factor depends on the coefficients of the selected regression.

Studies also show that MMI → PGA/PGV relationships vary by region (due to differences in building stock, local site conditions, and the way intensity is assessed), and that PGV often correlates better with higher damage levels. Atkinson and Kaka [38] derived MMI → PGA/PGV relations for the central United States and concluded that PGV-based metrics are more robust at higher intensities, while PGA-based relations remain useful, particularly when the objective is to estimate acceleration from observed intensity. Ultimately, MMI → PGA should be regarded as a statistical estimate with known dispersion. Contemporary studies extend this framework through ground-motion–to–intensity conversion equations (GMICEs), which commonly adopt segmented logarithmic forms and explicitly account for uncertainty (standard deviations). Caprio et al. [39] synthesise global and regionally calibrated relationships and demonstrate how strongly regionality influences both coefficients and applicability ranges. A key practical implication is that, when converting MMI to PGA (or vice versa), regionally appropriate coefficients should be used and the median together with an uncertainty range (e.g., ±σ) should always be reported, rather than a single "exact" value.

For consistent application, it is essential to specify the PGA component definition and the units used (e.g., the larger of the two horizontal components; expressed in g ili cm/s²), as well as the processing protocol adopted for peak-value determination. Departures from the assumptions under which the relationships were derived may lead to systematically biased estimates. Therefore, when reporting an estimated PGA, it is recommended to state the adopted component definition and units, together with the associated uncertainty range.

3.1.1.2. Did you feel it? (DYFI)

The USGS Did You Feel It? (DYFI) system is designed for rapid collection of macroseismic data from the public via online

questionnaires and mobile platforms, enabling the production of intensity maps immediately after an earthquake. The questionnaires record observed effects on people, objects, and buildings (e.g., felt shaking, falling objects, minor/major damage) together with the location of the report. Individual responses are first converted into numerical scores for each question and are then aggregated at the community level into the *Community Weighted Sum* (CWS). The *Community Decimal Intensity* (CDI), a continuous (decimal) intensity consistent with the MMI scale, is subsequently computed from CWS using a standard logarithmic function:

$$CDI = 3{,}40\ln(CWS) - 4{,}38 \quad (9)$$

The resulting value is rounded to one decimal place. If CWS > 0, a minimum value of CDI = 2.0 is assigned, while the overall CDI is capped at 9.0. The procedure is calibrated such that, at the community level, CDI on average corresponds to the MMI obtained through classical macroseismic assessment. This workflow makes it possible to transform a large number of heterogeneous qualitative descriptions into a quantified intensity measure for individual settlements or areas.

Mapping CDI → MMI yields an interval-based result (e.g., approximately 2.5–3.4 → MMI III, 3.5–4.4 → MMI IV, 4.5–5.4 → MMI V). Although the thresholds depend on the adopted rounding convention, the aim is to maintain compatibility with established intensity-mapping protocols and practice. It is important to emphasise that CDI and "traditional" MMI are not derived through identical procedures; some discrepancies are therefore expected, particularly in areas with few reports or atypical effects. While individual reports are of non-uniform quality (e.g., differences in how questions are understood, respondent bias, and varying digital reach), the general principle that "quantity compensates for quality" largely applies. When aggregated, CDI shows consistent agreement with instrumental ground-motion measures. Key limitations include uneven spatial coverage (controlled by population density and internet access) and the need for a minimum number of reports per spatial unit to obtain stable estimates.

The reliability of this approach stems from the statistics of large numbers. An individual report may be noisy, but an aggregated sample at the community level provides a stable and representative indicator of local shaking severity. Comparisons with instrumented ground-motion records show that DYFI-derived intensities correlate well with PGA/PGV and provide a useful quantitative basis for analyses and decision-making [40]. In this way, DYFI acts as a bridge between observed effects and engineering ground-motion metrics. For engineering applications, the key workflow is: responses → CWS → CDI → MMI → PGA. First, CDI is obtained from the collected responses, and CDI may then be translated into an integer MMI value if required. PGA is subsequently estimated from MMI using empirical intensity–ground-motion relationships. These relationships are logarithmic and have been derived from large datasets of recordings and observations [37], while more recent reviews provide global formulations and regionally calibrated variants [39].

A two-decade overview of the system highlights its speed, broad spatial coverage, and usefulness for risk communication and scientific analysis. It also emphasises methodological developments (e.g., improvements in the questionnaire, filtering, and visualisation) and international implementations. Recent studies further exploit multi-year CDI datasets, confirming that CDI and MMI are comparable and statistically consistent. Overall, DYFI provides an operationally rapid and scientifically robust source of macroseismic data; the key is the standardised conversion of heterogeneous public reports into CDI via CWS and a logarithmic formulation, accompanied by a reasonable treatment of uncertainty and reporting bias.

3.1.1.3. GMPE model (Ground-motion prediction equation)

A GMPE (Ground-Motion Prediction Equation) is a statistical model that, for a given earthquake and site, provides the expected level of ground motion (e.g., PGA, PGV, or PSA) together with the associated variability around that expectation. Mathematically, GMPEs predict the mean value in logarithmic space and the corresponding standard deviation, because recorded ground-motion amplitudes are approximately log-normally distributed. For specified inputs (e.g., M_w =6.5, R_{rup} = 15 km, strike-slip mechanism, v_{s30} = 360 m/s), a GMPE defines the median lnY i σ.

Each GMPE incorporates the moment magnitude M_w, one or more distance measures to the rupture (e.g., R_{rup}, R_{jb}, R_x) that capture source geometry; faulting style (strike-slip/normal/reverse); potential hanging-wall effects (asymmetry of motion on the hanging-wall side relative to the footwall); and site conditions represented by v_{s30}, including nonlinear amplification under strong shaking. Where required, additional parameters such as $Z_{1.0}$, or $Z_{2.5}$ (depth to specified shear-wave velocity horizons) are included to capture longer-period effects. These elements are standard in the so-called NGA-West2 set of relationships for active shallow crust (ASK14, BSSA14, CB14, CY14), which were developed using large strong-motion databases and are documented with clearly defined ranges of applicability.

Ground motions induced by earthquakes are not the same across different tectonic environments: active crustal regions (e.g., California, the Apennines), stable continental interiors, and subduction zones exhibit different attenuation characteristics and site-response effects. This is why regional GMPE families have been developed (e.g., NGA-West2 for active shallow crust; pan-European relationships based on the RESORCE database), and why practical applications often adopt weighted combinations of several suitable models to represent epistemic uncertainty and to ensure smooth transitions between regions and modelling assumptions [41].

Even without a single recording station, a GMPE (or a weighted set of GMPEs) can provide an initial (*a priori*) map of the median ground motion and its uncertainty, while accounting for local site effects. Once seismic recordings become available, this map is statistically adjusted toward the observations (measurements dominate near stations, whereas the model remains more influential farther away). In probabilistic seismic hazard analysis, GMPEs are the core component that links seismotectonic information to the engineering intensity measures needed for decision-making [42].

3.1.1.4. USGS ShakeMap system

ShakeMap is a USGS system that produces spatial maps of ground-motion intensity (PGA/PGV/PSA and MMI) immediately after an earthquake. It does so by computing an initial (*a priori*) ground-motion field from GMPEs, applying corrections for local site conditions (e.g., via V_{s30}), "anchoring" that field to recorded values from seismic stations, and, where appropriate, incorporating intensity observation points (MMI→PGA/PGV via GMICE). These inputs are then fused within a statistical framework to obtain an updated (*posterior*) ground-motion field, typically expressed in terms of the median and associated uncertainty.

The Petrinja earthquake was a shallow event occurring within the active crust of the Euro-Mediterranean seismotectonic domain. In the ShakeMap configuration for such events, a GMPE set for active shallow crust is typically adopted, most commonly a combination of four NGA-West2 models (developed on large strong-motion datasets) together with several pan-European relations. In practice, this results in a seven-model suite: NGA-West2 (active shallow crust) models, ASK14 [43], BSSA14 [44], CB14 [45], and CY14 [46], supplemented by regionally calibrated Euro-Med models [47–49], developed primarily using the RESORCE/ESM datasets and tailored to Europe and the Middle East. This combination is consistent with what ShakeMap describes as the GMPE set for active shallow crust outside the United States, blending "global" NGA-West2 relations with regional Euro-Mediterranean models to capture both the breadth of available data and regional nuances in attenuation and site effects. High weights of 0.35 are assigned to the regional Euro-Mediterranean models [48, 49], which were developed using the RESORCE/ESM Euro-Mediterranean datasets and are specifically intended to represent active shallow crust in Europe an the Middle East; they are therefore the most relevant for Croatia and the surrounding region. A moderate weight is assigned to the independent Japanese ASC model [47] to address epistemic uncertainty; this model receives a weight of 0.10 as an alternative active shallow crust branch based on the exceptionally rich Japanese dataset of shallow earthquakes. Including a "non-regional" ASC model with a moderate weight helps represent epistemic uncertainty without allowing such a model to dominate the median estimate. Small weights of 0.05 each are distributed across the four NGA-West2 relations [43–46], which are widely accepted global models. This weighting strategy, favouring "local" models, is fully consistent with recommendations for assembling GMPE suites outside the United States, where regional models should dominate combined sets. In this way, the model suite maintains a "bridge" to globally established relations while ensuring that the regional Euro-Mediterranean models are not suppressed. The resulting GMPE curves and associated standard deviations for the Petrinja earthquake, together with the recorded data and DYFI indicators, are shown in Figure 4.

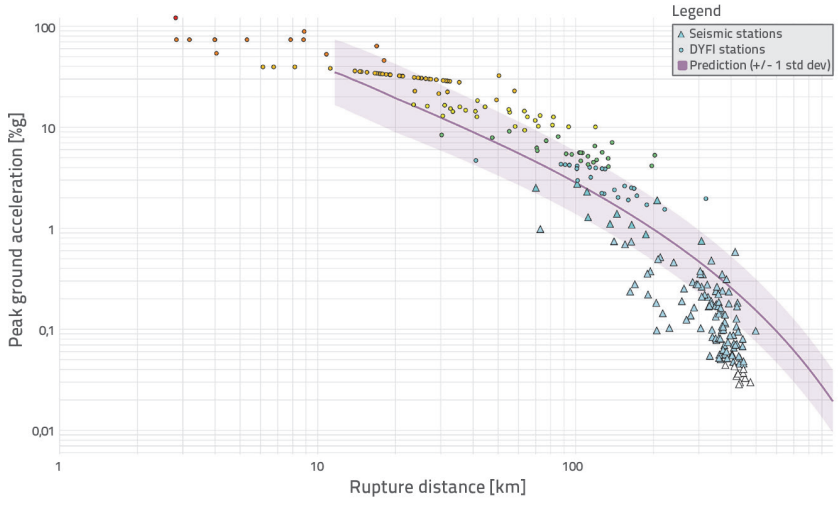

Figure 4. USGS-based peak ground acceleration (PGA) estimates: GMPE prediction (thick purple line) and observations (seismic stations—blue triangles; Did You Feel It (DYFI)—coloured circles), accounting for local site conditions [36]

3.1.1.5. Determining PGA from the ShakeMap system

For each earthquake, the ShakeMap system ingests the event magnitude, location and, where available, fault geometry, together with all available instrumental data (PGA/PGV/PSA from seismic stations). The system is connected to operational seismic platforms (Antelope, SeisComP3, AQMS), so station measurements are received automatically along with station identifiers and standard metadata.

The first step is the construction of an initial ground-motion field using GMPEs. The event is classified into an appropriate tectonic regime, a corresponding GMPE set and model weights are selected, and a suite of relations is thus defined to provide the median and dispersion of ground motion away from observation points. All model predictions and station data are normalised for local site conditions using the time-averaged shear-wave velocity in the upper 30 m (v_{s30}). For v_{s30}, ShakeMap most commonly relies on USGS topographic maps and proxy models [50], although locally measured shear-wave velocities can be used where available. Where needed, additional parameters (e.g., $Z_{1.0}/Z_{2.5}$, the depths to V_s = 1.0 and and 2.5 km/s, respectively) may also be included. For peak-motion maps, ShakeMap explicitly reports the larger of the two horizontal components, rather than a vector sum or geometric mean. This definition is applied consistently both when ingesting station values and when computing predictions from GMPEs. From the selected model suite, ShakeMap forms a weighted average in logarithmic space: for each grid point, it combines the medians and dispersions of individual GMPEs into a single initial (*a priori*) median PGA and an associated standard deviation σ. In this way, the approach simultaneously leverages regionally appropriate relations and globally established reference models, thereby reducing epistemic uncertainty prior to incorporating the station observations.

Measured PGA values from seismic stations enter the system as point

measurements with relatively low uncertainty. In parallel, MMI/DYFI and other field-based intensity assessments, where available, are converted to PGA via GMICEs and incorporated with higher uncertainty than instrumental observations. In this way, ShakeMap integrates both what was recorded by instruments and what was experienced and observed in the field, while applying a clear hierarchical weighting that reflects data quality.

In the final step, ShakeMap reconciles all available information by conditioning the *a priori* PGA field derived from the GMPE suite on actual observations: point-based station PGA values (assigned high weight) and, where available, MMI/DYFI points converted to PGA via GMICEs (assigned lower weight). A smoothly varying spatial correlation is assumed (nearby points are more similar than distant ones), and the resulting fields are obtained through Gaussian, kriging-like interpolation. Locally, the map is adjusted the measured peak values, while the areas between observation points are filled in a physically reasonable manner guided by the initial spatial model. The outcome is an updated (*posterior*) field that provides two pieces of information at each grid node: the median PGA as the best estimate and the standard deviation σ as the associated uncertainty. Near stations, the estimate is tightly anchored to the measurements and σ is small; with increasing distance from data, values smoothly revert toward the initial GMPE-based field and σ increases. The outputs include maps of PGA/PGV/PSA/MMI as well as uncertainty maps, together with digital raster/vector products suitable for GIS and further analyses. The peak ground acceleration map for the Petrinja earthquake obtained using this methodology is shown in Figure 5.

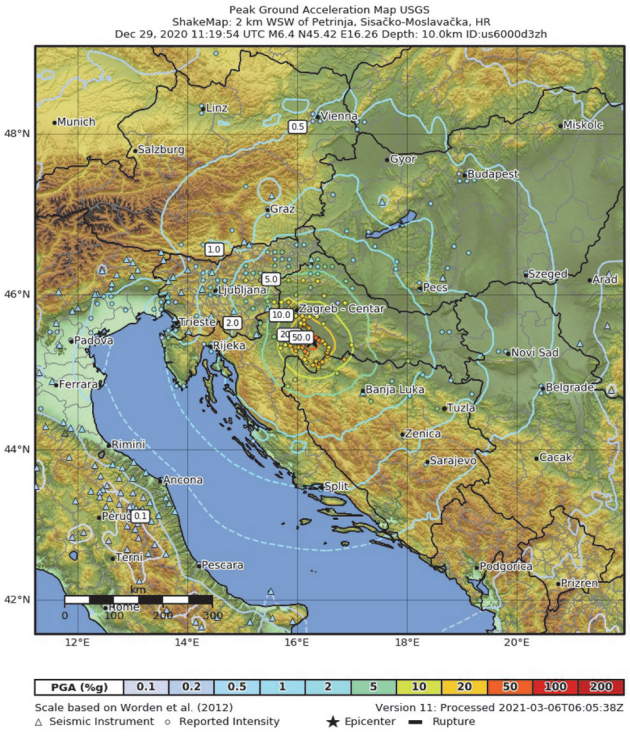

Figure 5. Peak ground acceleration map for the 2020 Petrinja earthquake according to the ShakeMap system, taken from [36]

3.1.1.6. Recommendation for selecting peak ground acceleration for the 2020 Petrinja earthquake

During the Petrinja earthquake, the nearest seismic stations were located at distances of approximately 50 km from the epicentre, and at those locations the ShakeMap estimates already agree well with the instrumental recordings. With such station geometry, the updated (*posterior*) field in the central part of the affected area necessarily closely resembles the initial (*a priori*) field derived from the GMPE suite. If very high MMI/DYFI points, converted to PGA via the GMICE procedure, are additionally included, their cumulative effect can easily produce unrealistically high peaks on the map within the epicentral zone. Given the large and strongly nonlinear uncertainty of GMICE at high intensities (VIII–IX) and short distances, it is more reasonable for engineering assessments in the Petrinja area to omit MMI/DYFI inputs and rely on the GMPE-based field.

A suite of regionally appropriate GMPEs (Euro-Mediterranean relations combined with the reference NGA-West2 models) provides a stable median with realistic near-field saturation and well-defined uncertainty (σ). However, the quality of this field depends critically on local site conditions: generic v_{s30} values inferred from topography [50] are often a coarse approximation in lowland, alluvial, or filling settings such as the Petrinja area. Using locally measured $v_{s30,}$ for example from surface-wave methods such as SASW or MASW, or from downhole geophysical measurements, replaces the generic proxy with site-specific geotechnical/geophysical data and reduces systematic site-amplification errors that can lead to overestimation of peak ground acceleration on soft deposits.

The combination of GMPE-based predictions and locally measured v_{s30} values therefore provides the most robust basis currently available. It respects near-field physics through validated functional forms and saturation behaviour, is consistent with the component definition reported by ShakeMap (the "larger of the two horizontals"), and varies spatially according to measurable site properties rather than reporting biases. The resulting PGA field has a transparent, quantitatively defined uncertainty and avoids artificial irregularities that can arise in the epicentral area when numerous intensity points are introduced without nearby instrumental constraints. For engineering applications, especially rapid liquefaction-potential screening, PGA defined in this manner provides an appropriate input parameter: the GMPE median and quantiles, locally adjusted using measured or reliably estimated v_{s30} values, yield conservative and stable estimates for calculating the cyclic stress ratio (CSR). In the Petrinja case, selecting an appropriate GMPE suite in combination with locally constrained v_{s30} conditions minimises methodological bias and maximises the use of genuinely available data.

Figure 6 presents the peak ground acceleration map for the Petrinja earthquake obtained using the selected median PGA value increased by one standard deviation. The site-amplification correction was based on the globally available v_{s30} map [50], which should be updated in future work using locally available v_{s30} values derived from the numerous geophysical investigations.

A further contribution to understanding local site conditions is provided by the study of Stanko and Markušić [51], who developed a nonlinear site-amplification model for Croatia based on the

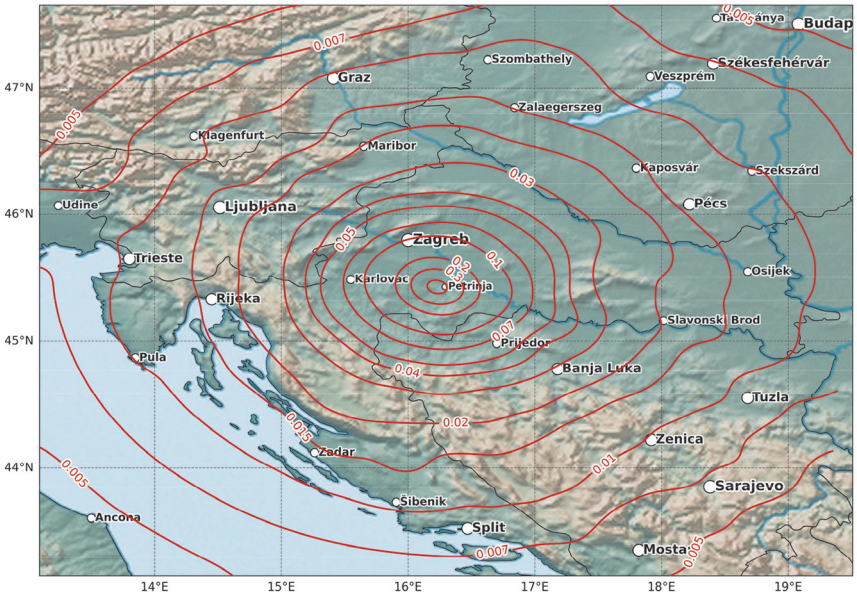

Figure 6. Map of PGA distribution for the Petrinja earthquake based on the GMPE-derived median peak ground acceleration increased by one standard deviation

parameters $v_{s,30}$, T_0 (the dominant site period), and H_{800} (depth to bedrock), as well as the intensity of the input rock motion, consistent with the Eurocode 8 soil classification and its revised provisions. The proposed model represents a significant step forward for seismic hazard assessment in regions with sparse strong-motion data, such as Croatia, and raises the question of how the Petrinja earthquake may influence future hazard calculations.

In the context of selecting representative peak ground acceleration values for the Petrinja earthquake, the study by Markušić et al. [52] is particularly noteworthy. The authors evaluated the USGS ShakeMap by examining the attenuation of peak horizontal acceleration in the Dinarides using the relations of Herak et al. [53] and Markušić et al. [54], calibrated for rock or very stiff soil conditions. In addition, they considered three global empirical ground-motion prediction equations (GMPEs) deemed potentially applicable to the region. The authors concluded that the estimated PGA values for the Mw 6.4 event in the near-epicentral zone (within 10 km) substantially exceed the seismic-hazard expectations for return periods of 95 and 475 years, while being comparable to values associated with a 1000-year return period. These findings confirm the exceptional significance of this earthquake in the context of the region's historical seismicity, and they raise an important question regarding its implications for future seismic-hazard calculations, not only for the epicentral area, but also for the wider Zagreb region, which is home to more than one million inhabitants.

3.1.2. Determining soil resistance (CRR) from in-situ tests

Within the cyclic stress approach, the assessment of soil resistance to liquefaction is based on the soil's ability to maintain shear strength under cyclic loading. In practice, this resistance, expressed as the cyclic resistance ratio (CRR), is most commonly estimated from in-situ field tests. The principal tests include the standard penetration test (SPT), the cone penetration test (CPT), and measurements of shear-wave velocity (v_s), with dilatometer tests (DMT) and dynamic probing (DPL/DPSH) sometimes used as alternatives or complementary methods. These data provide the basis for empirical

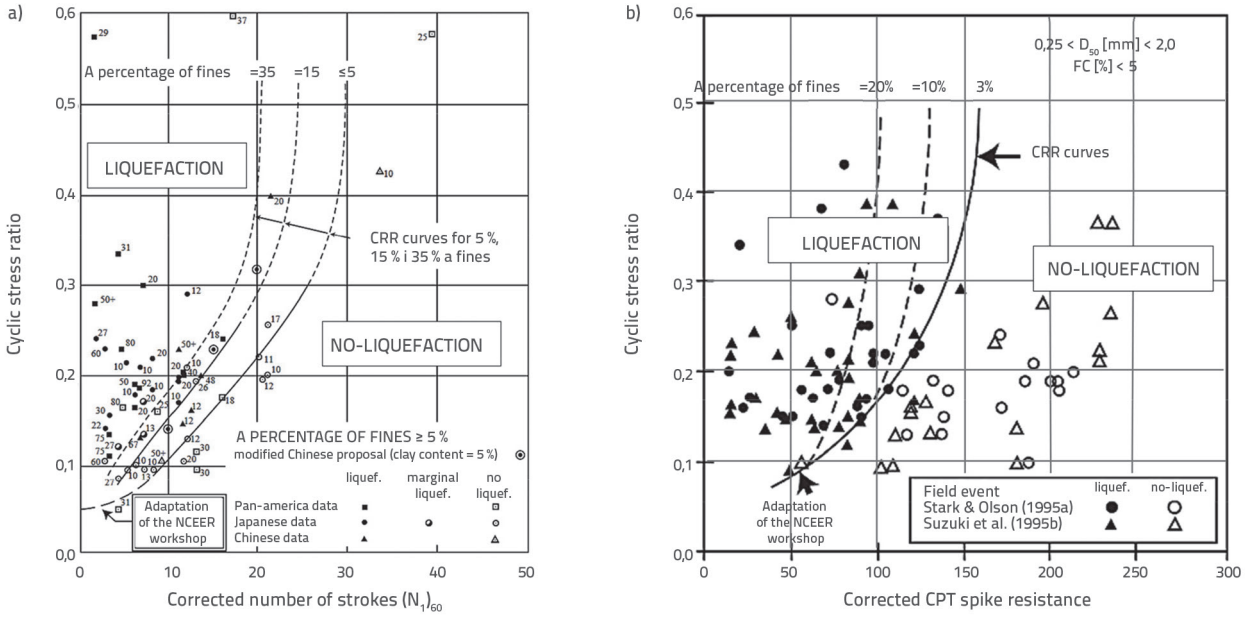

Figure 7. Example liquefaction triggering charts based on: a) SPT; b) CPT results, modified after [59]

correlations used to quantify cyclic resistance. According to the current EN 1998-5 standard [55], investigations for liquefaction potential assessment must, as a minimum, include either SPT or CPT testing and laboratory determination of the particle-size distribution of representative samples. The standard also specifies conditions under which liquefaction may be neglected based on SPT results: if the sand contains more than 20 % clay and the plasticity index exceeds 10, if the fines content in the sand exceeds 35 % and the corrected SPT blow count $(N_1)_{60}$ is greater than 20, or if the material is clean sand with $(N_1)_{60} > 30$. In these cases, pore-pressure generation during earthquake loading is expected to be limited, and shear strength is maintained at levels that prevent liquefaction triggering.

Building on the observation that increasing relative density leads to higher SPT penetration resistance as well as greater liquefaction resistance, Seed et al. [56] were the first to propose an empirical relationship between the SPT blow count and CSR. This work provided the basis for the earliest liquefaction triggering charts [57] and for the development of practical procedures to evaluate cyclic resistance (Figure 7a). The curves in that figure represent liquefaction resistance for clean sand and divide the domain into a region where liquefaction is possible (above the curve) and a region where liquefaction is not expected (below the curve). A family of resistance curves is defined as a function of fines content in cohesionless soils. Several authors subsequently proposed modifications to these curves [58, 59].

When CPT testing is used to assess liquefaction potential (Figure 7b), the most commonly employed parameter is the CPT cone tip resistance, or more specifically the derived parameter of equivalent clean-sand penetration resistance, (q_{c1Ncs}). It should be noted that current practice most often relies on three CPT-based procedures for evaluating liquefaction resistance from CPT data: Moss et al. [60], Robertson [61], and Boulanger and Idriss [33]. The details of each procedure are provided in the literature, and the methods are periodically updated.

An alternative approach for liquefaction potential assessment is the use of shear-wave velocity (v_s) data to construct liquefaction triggering relationships [62]. In practice, this method has been applied less frequently than conventional SPT- or CPT-based procedures. Reliable (v_s) values can be obtained from detailed, but more costly and time-consuming, downhole measurements, whereas surface-wave methods such as MASW provide a faster and more economical option. Although surface seismic measurements require calibration against laboratory and SPT/CPT data, they enable liquefaction screening over larger areas, which is particularly useful when the objective is the preliminary identification of broader zones of potential risk.

3.2. Liquefaction potential assessment at two representative sites in Sisak–Moslavina county

To illustrate the procedure used to assess liquefaction potential in Sisak–Moslavina County, two representative sites were analysed in this study. The first site is located in Makančeva Street in Petrinja, approximately 750 m from the Petrinjčica River and about 1,000 m from the Kupa River. At this location, pronounced liquefaction occurred during the 2020 Petrinja earthquake, manifested by sand ejecta and documented surface deformations. The second site is situated in Frano Kršinić Street in Sisak, within an area designated for the construction of a multi-storey residential building, approximately 800 m from the Kupa River, where no liquefaction was observed during the earthquake. Both sites are indicated in Figure 1. The selection of these two locations is based on the fact that both feature sandy layers below the groundwater table, but with a key difference in their relative density. This enables a meaningful comparison between the conditions that led to liquefaction in Petrinja and those in Sisak where triggering did not occur, providing an evidence-based insight into the parameters that control the liquefaction response of the ground.

At both sites, exploratory boreholes were performed and cone penetration tests (CPT) were carried out to a depth of 10 m. The resulting profiles of CPT cone tip resistance (q_c) and sleeve friction (f_s) are shown for Makančeva Street in Figure 8 and for Kršinić Street in Figure 9. The same figures also present the soil classification profile determined according to Robertson [63], based on the soil behaviour type index (SBTn). The cone resistance profiles show relatively lower resistance values down to depths of about 3–4 m, corresponding to alternating clayey layers and silty mixtures. Below this zone, sandy deposits extend to greater depths (to about 8 m at the Makančeva Street site and to 10 m at the Kršinić Street site), with locally higher cone resistance values at Makančeva Street and consistently higher cone resistance values at Kršinić Street. It should be emphasised that, using the average q_c value for the sand layer, the equivalent clean-sand cone resistance q_{c1Ncs} was calculated using the following expression:

$$q_{c1Ncs} = q_{c1N} + \Delta q_{c1N} \tag{10}$$

where:

$$q_{c1N} = C_N \cdot \frac{q_c}{p_a} \tag{11}$$

in which C_N is the overburden (stress) normalisation factor and p_a is atmospheric pressure. The equivalent clean-sand correction Δq_{c1N} is calculated using:

$$\Delta q_{c1N} = \left(11{,}9 + \frac{q_{c1N}}{14{,}6}\right) exp\left(1{,}63 - \frac{9{,}7}{FC+2} - \left(\frac{15{,}7}{FC+2}\right)^2\right) \tag{12}$$

Here, FC denotes the fines content, which in the present example is estimated using the expression proposed by Kovačević et al. [64]:

$$FC = 17{,}45 \cdot I_c^{1{,}662} - 35{,}42 \tag{13}$$

Where I_c is the soil behaviour type index. The equation is applicable within the range $1.40 \le I_c \le 3.42$.

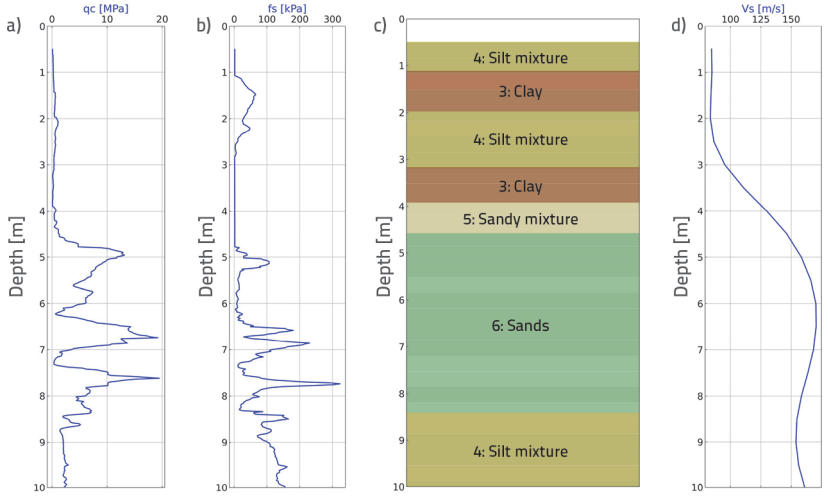

Figure 8. Raw CPT cone tip: a) resistance; b) sleeve friction; c) profiles for the Makančeva Street site in Petrinja, with the corresponding SBTn soil classification profile; d) the shear-wave velocity profile

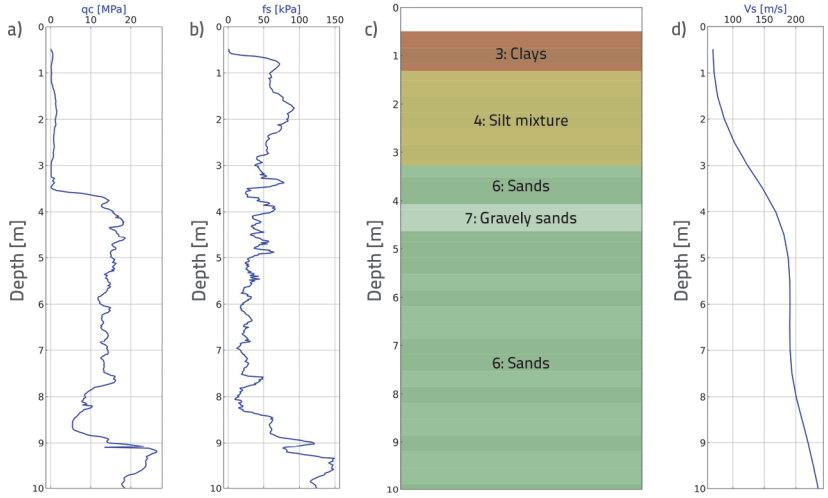

Figure 9. Raw CPT cone tip: a) resistance; b) sleeve friction; c) profiles for the Kršinićeva Street site in Sisak, with the corresponding SBTn soil classification profile; d) the shear-wave velocity profile

In the CSR calculations, peak horizontal ground acceleration was used, considering two variants: (i) values extracted from the USGS ShakeMap [36] for each site, where site amplification was defined using the global $v_{s,30}$ proxy model [50]; and (ii) values obtained from the empirical GMPE-based approach adopted in this study, with site amplification derived from the measured shear-wave velocity profiles shown in Figures 8d and 9d. The computed $v_{s,30}$ at the Makančeva Street site is 187 m/s, which, according to EN 1998-1 [34], places the ground at the boundary between Soil Types D and C, whereas at the Kršinićeva Street site $v_{s,30}$ = 282 m/s, corresponding to Soil Type C. As discussed above, the GMPE-based approach typically yields lower peak horizontal accelerations than those suggested by ShakeMap.

The liquefaction potential analysis for the Makančeva Street site (Figure 10), presented on the Boulanger and Idriss triggering chart [59], reveals pronounced differences in the inferred CSR depending on the selected method for defining peak ground acceleration. Using ShakeMap inputs yields exceptionally high CSR values, implying a strong potential for liquefaction triggering. In contrast, the values obtained using the GMPE-based approach also indicate possible liquefaction, but with lower computed CSR, which is more consistent with evidence from global databases of documented liquefaction cases at other sites worldwide.

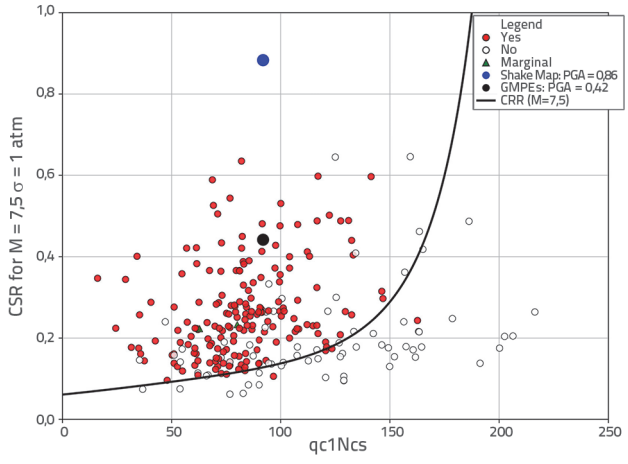

Figure 10. CPT-based liquefaction triggering chart for the Makančeva Street site in Petrinja, where liquefaction occurred

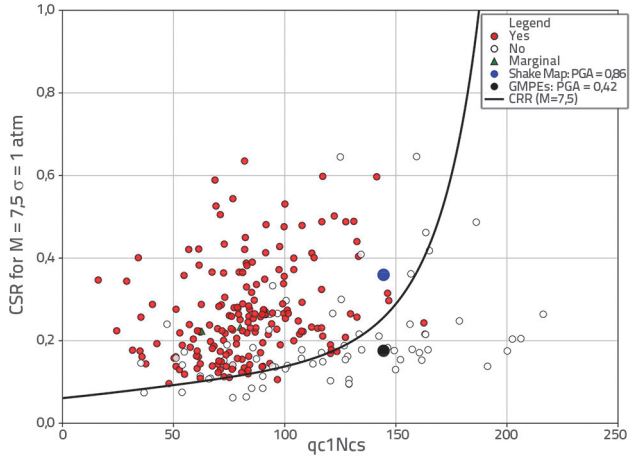

Figure 11. CPT-based liquefaction triggering chart for the Kršinić Street site in Sisak, where liquefaction did not occur

For the location in Kršinićeva Street (Figure 11), where no liquefaction was recorded during the Petrinja earthquake, the situation is analogous: ShakeMap peak ground acceleration values place the site within a zone of potential liquefaction, whereas the application of the GMPE model with a locally determined V_{s30} value classifies the site as non-liquefiable. This example highlights that the use of GMPE models in combination with locally measured V_{s30} values provides a more realistic and consistent assessment of soil liquefaction potential in accordance with empirical evidence, and reduces the risk of hazard overestimation in the context of local geotechnical conditions.

4. Ground-Improvement technologies applied during post-earthquake reconstruction

Decisions on whether ground improvement was required after the 2020 Petrinja earthquake were largely governed by the post-earthquake assessment of liquefaction potential at individual sites. For most replacement (new) single-family houses and buildings, geotechnical investigations indicated that the liquefaction risk was relatively low, which was expected given that replacement sites were selected to avoid areas known for loose alluvial sediments, high groundwater levels, or previously documented liquefaction manifestations. Consequently, in the majority of cases it was possible to design foundations on natural ground without the need for special ground-improvement measures.

The opposite situation was observed for existing residential buildings, where liquefaction manifested during the earthquake through differential settlements, overall settlements, lateral displacements, cracking, and local loss of bearing capacity. Because ground remediation was necessary for such structures as part of structural rehabilitation, a range of ground-improvement technologies was applied, with particular emphasis on low-pressure injection. The most commonly used techniques were compaction grouting with cement suspensions and injection of expanding chemical resins, aimed at increasing density and reducing deformability of loose strata while minimising disturbance to existing structures and connected utilities. These technologies proved suitable due to their ability to achieve precise, localised treatment and the relatively high level of execution control.

However, it is important to note that, despite clear warnings from the geotechnical community that high-quality seismic reconstruction is not possible without ground improvement, a portion of buildings located in areas with confirmed liquefaction still did not undergo appropriate ground-remediation works, primarily as a result of decisions made by the owners themselves.

For infrastructure assets, the situation was considerably more complex. Levees along the Kupa, Sava, Glina, and Maja rivers, which experienced significant deformations and local failures during the earthquake, are situated on extensive alluvial plains where deep and laterally continuous layers of potentially liquefiable soils are a natural geological feature. For such linear structures, relocation is not an option, and their flood-protection function requires a high level of safety. Accordingly, based on comprehensive geotechnical and geophysical investigations, it was confirmed that liquefaction potential remains high and that ground-improvement measures are necessary. The selected improvement methods were tailored to the depth and characteristics of the liquefiable layer (Figure 12). Where potentially liquefiable layers occur at greater depths, jet-grouting columns were adopted, allowing the formation of continuous cylindrical zones of improved ground and a substantial increase in shear strength. For shallow, loose liquefiable layers, dynamic compaction methods were applied, enabling effective densification and a reduction in the potential for pore-pressure build-up. Detailed discussions of the challenges and specificities of rehabilitating such infrastructure systems are provided by Mihaljević and Zlatović [29] and Bačić et al. [65].

The literature also reports case studies of specific ground-improvement measures implemented in the post-earthquake period, such as the remediation of foundation soils beneath the Gromova Bridge on state road DC37 (section 1 at chainage km 0+126) across the Kupa River [66], which involved the use of jet-grouting columns. Bago et al. [67] highlight the benefits of previously installed stone columns beneath the tank area of the Sisak Terminal, which during the earthquake facilitated the dissipation of excess pore pressures and thereby likely prevented liquefaction that might otherwise have occurred due to the presence of loose sandy deposits at the site.

5. Strategic directions for future liquefaction research in Sisak–Moslavina County

According to the AASHTO guidelines [68], a confirmed occurrence of liquefaction in the immediate vicinity of an area is a clear indicator that a detailed assessment of the entire affected zone is required. It was precisely such manifestations following the Petrinja earthquake that triggered the systematic collection of a large body of geological, geotechnical, and geophysical data, generated through scientific projects as well as engineering and professional activities. This growing knowledge base offers an exceptional opportunity to introduce a unified, standardised methodology for liquefaction-potential mapping, applicable not only in Sisak–Moslavina County but also across the entire

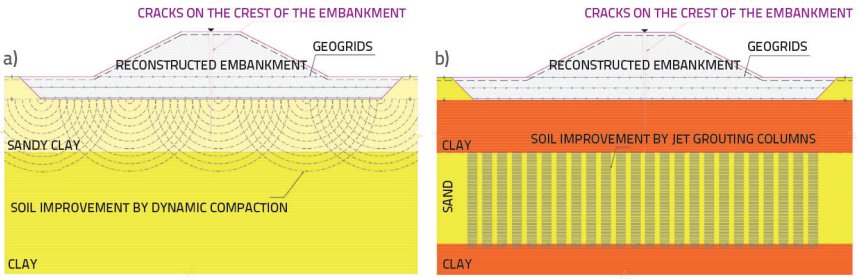

Figure 12. Cross-sections of levees with ground-improvement measures: a) dynamic compaction; b) jet-grouting columns

territory of the Republic of Croatia, and to integrate it as a core component of comprehensive seismic microzonation.

The fundamental objective of liquefaction microzonation is to synthesise existing knowledge and optimise future field investigations through a multi-level assessment framework, ranging from lower-resolution preliminary susceptibility screening to detailed site-specific analyses. The concept should be grounded in the principle of progressive uncertainty reduction: as the level of detail increases, the range of plausible interpretations narrows and the reliability of risk estimates improves. Depending on the required level of detail and project needs, the methodology can be divided into three tiers:

At the lowest-resolution level (Tier 1), general susceptibility maps should be refined using data from geological maps, geomorphological analyses, high-resolution terrain models, hydrological datasets, and all available information on groundwater levels. It is particularly important to emphasise that the preliminary liquefaction map [14], produced immediately after the earthquake, represents a valuable baseline that should be methodologically expanded and upgraded by incorporating newly available data. Such maps serve as an initial screening tool, delineating areas where the basic preconditions for liquefaction are met and where more detailed investigations are required;

At the detailed methodological level (Tier 2), a dense network of geotechnical investigations is integrated, primarily CPT soundings and borehole investigations including SPT, together with data from surface-based geophysical methods, with particular emphasis on seismic techniques. The ISSMGE guidelines [65] emphasise that such detailed geotechnical investigations form the basis for producing high-resolution seismic microzonation maps. The resulting spatial resolution is suitable for spatial-planning documents and strategic risk management. At this stage, groundwater depth maps are also commonly employed, as they represent a critical input for liquefaction-potential calculations. It is therefore recommended to establish a piezometric network and a programme of continuous groundwater-level monitoring in order to ensure reliable, long-term hydrogeological trends. For the development of Tier 2 maps, appropriate detailed seismic-hazard inputs must also be defined, while zoning can be performed using factors of safety against liquefaction, for example via the cyclic stress approach, or through probabilistic estimates of liquefaction occurrence;

The most comprehensive mapping level (Tier 3) is intended for individual engineering interventions and projects. It encompasses targeted investigations required to support robust design decisions, particularly for infrastructure assets, facilities critical to community functionality, and critical segments of linear infrastructure systems. At this tier, a combination of field testing and applied dynamic laboratory testing is essential, and nonlinear dynamic analyses are desirable for the seismic-hazard input. Only at this level can mitigation measures be designed with sufficient confidence. Linear infrastructure, such as embankments, roads, and railways, poses a particular challenge because spatial soil variability is often very pronounced. The literature indicates that point-based investigations alone frequently cannot adequately capture the inherent spatial heterogeneity of the ground. In this context, a valuable contribution is offered by the approach developed within the LeveeLiq project [70], which focuses on estimating the spatial distribution of liquefaction potential at the scale of the infrastructure asset itself. The approach accounts for both vertical and horizontal variability and integrates results from multiple in-situ methods, primarily CPT and MASW, supported by occasional borehole data. LeveeLiq develops algorithms for automated estimation of the spatial probability of liquefaction, including detrending of the collected data, statistical processing, definition of spatial-variability parameters, and generation of log-normally distributed spatially correlated random fields. This yields a realistic representation of the spatial (linear) distribution of liquefaction potential and enables remediation measures to be optimally tailored to the actual ground conditions.

In developing the proposed multi-tier methodology, it is important to consider international experience and existing formalised approaches to seismic microzonation in countries with elevated seismicity [69, 71–74]. These experiences clearly indicate that reliable high-resolution mapping must integrate geological basemaps, geotechnical and geophysical information, key hydrogeological parameters, and a consistent seismic input. A particularly valuable example of European practice is the H2020 LIQUEFACT project [2], whose holistic framework is focused on multi-criteria risk evaluation and the production of geospatial liquefaction-susceptibility maps. Project researchers emphasise [75] the need for a multi-level approach to liquefaction-potential mapping, which can be directly related to the three-tier concept outlined above. While the project demonstrated the potential for large-scale mapping, it also highlighted that liquefaction is a highly localised phenomenon and that regional maps cannot replace detailed site-specific geotechnical investigations. Such maps should therefore be viewed as a strategic decision-support tool rather than as a final basis for design.

Future liquefaction research should also include the systematic organisation of datasets used to calibrate existing global empirical liquefaction triggering charts and models for estimating liquefaction resistance. Reliable application of such charts requires high-quality information on peak ground acceleration, particle-size distribution, relative density, groundwater depth, and CPT/SPT/ v_s test results. A systematic and standardised data structure would enable long-term updating of susceptibility maps.

In this context, one of the key prerequisites for a reliable liquefaction-potential assessment is the use of consistent seismic input parameters. For the Petrinja earthquake, the most appropriate peak-acceleration values are those derived from a GMPE-based approach, using the median and relevant quantiles, locally adjusted using actual v_{s30} values. This framework provides conservative and stable inputs for cyclic stress ratio (CSR) calculations, minimises bias, and maximises the use of the most reliable available information.

6. Conclusion

The 2020 Petrinja earthquake represents the largest confirmed large-scale liquefaction event in Croatia to date, affecting an area of approximately 600 km² within a radius of about 20 km from the epicentre. Liquefaction manifestations were spatially distinct, occurring mainly as linear sand-ejecta features accompanied by straight ground fissures, deformations and settlements of roadways, damage to levees, and the destabilisation of bridges and other infrastructure. The highest concentration of phenomena was recorded along the Kupa, Sava, and Glina rivers, where recent alluvial deposits predominantly comprise clean sands, locally silty or gravelly sands, and occasional lenses of coarse gravel.

In the post-earthquake period, numerous scientific and professional investigations were carried out to document, understand, and quantify liquefaction occurrence, as well as to develop assessment and remediation approaches. The initial phase included compiling an inventory of liquefaction manifestations and producing preliminary susceptibility maps based on heuristic procedures and the available information on geological setting, groundwater conditions, and seismic excitation. Subsequent studies involved advanced geotechnical and geophysical investigations at selected representative sites, aimed at characterising soil properties, layer thicknesses, and cyclic resistance. The resulting datasets enabled calibration of empirical procedures and a more reliable interpretation of local ground conditions.

In parallel with research activities, extensive professional work was undertaken to support the reconstruction of existing structures and the construction of new residential and infrastructure facilities. Given the large number of sites, a rapid simplified cyclic stress approach, combined with empirical liquefaction triggering charts, was adopted to provide reliable estimates of the factor of safety and the probability of liquefaction. As a key input for defining seismic demand, the use of a GMPE-based framework in combination with locally measured (v_{s30}) values is recommended in order to ensure conservative, stable, and physically grounded inputs for CSR calculations.

Liquefaction-potential mapping, as an integral component of seismic microzonation, should be developed through multiple tiers, taking into account guidance from established international frameworks. At the basic, low-resolution level, the use of geological maps, geomorphological analyses, topographic models, and available groundwater information is recommended to identify potentially critical areas. At the more detailed level, where data coverage is denser, CPT, SPT, and geophysical investigations should be integrated to improve spatial resolution and increase the reliability of the assessment. At the local, most advanced level, particularly for infrastructure assets, it is necessary to address both vertical and horizontal soil variability and to apply a combination of field and laboratory methods to support robust design decisions.

Successful implementation of a three-tier liquefaction-potential mapping methodology requires clearly defined standards, unified data formatting, and the establishment of a national database of field and laboratory test results. Such a database would ensure long-term sustainability and allow continuous refinement of maps as new data become available. Overall, these considerations point to the need for a systematic, multi-level approach that combines broad geospatial screening with detailed in-situ investigations. Implemented in this way, the methodology would support rational risk management, enhance the reliability of liquefaction-potential assessment, and contribute to improving the resilience of Croatia's built environment to future earthquakes.

In addition, the use of locally collected data on geological structure, particle-size distribution, groundwater levels, and in-situ test results is recommended for the calibration and validation of global empirical liquefaction triggering charts. Such an approach enables domestic experience and documented liquefaction sites to be incorporated into international databases, thereby contributing to their continuous improvement.

Acknowledgements

This research was funded by the Croatian Science Foundation (HRZZ) under project IP–2022–10-7608, LeveeLiq (Mapping the spatial variability of liquefaction potential below the levees and modelling of optimal mitigation measures).

REFERENCES

[1] EM-DAT: The International Disasters Database, URL: www.emdat.be (accessed on September 15th, 2025)

[2] LIQUEFACT Project, HORIZON 2020 GA 700748, URL: www.liquefact.eu (accessed on September 17th, 2025)

[3] Bačić, M., Ivšić, T., Kovačević, M.S.: Geotechnics as an unavoidable segment of earthquake engineering, Građevinar, 70 (2020) 12; pp. 923–936, https://doi.org/10.14256/JCE.2968.2020

[4] Towhata, I.: Liquefaction Mitigation Measures: A Historical Review, in: Sitharam, T. G., Jakka, R., Kolathayar, S. (Eds.), Latest Developments in Geotechnical Earthquake Engineering and Soil Dynamics, Springer Transactions in Civil and Environmental Engineering, 2021, pp. 41–86, https://doi.org/10.1007/978-981-16-1468-2

[5] Ishihara, K., Okada, S.: Effects of stress history on cyclic behavior of sand, Soils and Foundations, 18 (1978), pp. 31–45, https://doi.org/10.3208/sandf1972.18.4_31

[6] Suzuki, T., Toki, S.: Effects of preshearing on liquefaction characteristics of saturated sand subjected to cyclic loading, Soils and Foundations, 24 (1984), pp. 16–28, https://doi.org/10.3208/sandf1972.24.2_16

[7] Olson, S.M., Green, R.A., Obermeier, S.F.: Geotechnical analysis of paleoseismic shaking using liquefaction features: a major updating, Engineering Geology, 76 (2005), pp. 235–261, https://doi.org/10.1016/j.enggeo.2004.07.008

[8] Wang, S., Yang, J., Onyejekwe, S.: Effect of previous cyclic shearing on liquefaction resistance of Mississippi River Valley silt, Journal of Materials in Civil Engineering, 25 (2013), pp. 1415–1423, 10.1061/(ASCE)MT.1943-5533.000069

[9] Seed, H.B., Idriss, I.M.: Analysis of Soil Liquefaction: Niigata Earthquake, Journal of the Soil Mechanics and Foundations Division, 93 (1967), 3, pp. 83–108, 10.1061/JSFEAQ.0000981

[10] Veinović, Ž.: Ocjena mogućnosti pojave likvefakcije i definiranje osnove za likvefakcijsko zoniranje na teritoriju Republike Hrvatske, dissertation, Rudarsko-geološko-naftni fakultet, Zagreb, 2007, 332 pp.

[11] Mijic, Z., Zlatović, S., Montgomery, J., Mijić, Z., Gjetvaj, V.: Liquefaction effects in the 2020 Mw 6.4 Petrinja, Croatia Earthquake, Soil Dynamics and Earthquake Engineering, 193 (2025), Article 109262, 10.1016/j.soildyn.2025.109262

[12] Torbar, J.: Izvješće o zagrebačkom potresu 9. studenoga 1880., Djela JAZU, knj. 1, VIII+141 str., 1882, Zagreb

[13] Pikija, M.: Basic Geological Map of SFRJ 1:100 000 scale, Sisak sheet, Federal Geological Survey of Yugoslavia, 1987

[14] Rudarsko-geološko-naftni fakultet Sveučilišta u Zagrebu: Studija o seizmički induciranim efektima Petrinjske potresne serije 2020-2021 – preliminarna identifikacija rizika, Knjiga: Kartografski podaci o likvefakciji, klizištima, podzemnoj vodi i urušnim vrtačama u GIS-u kao tematski slojevi prirodnih ograničenja vezanih uz tlo za primjenu u prostornom planiranju, Zagreb, 2021.

[15] Ministarstvo graditeljstva, prostornoga uerđnja i državne imovine: Informacijski sustav prostornog uređenja (ISPU), https://ispu.mgipu.hr/

[16] Tomac, I., Zlatović, S., Athanasopoulos-Zekkos, A., Bleiziffer, J., Domitrović, D., Frangen, T., Gjetvaj, V., Govorcin, M., Grilliot, M., Gukov, I., Herak, M., Hrženjak, P., Hutchinson, T., et al.: Geotechnical Reconnaissance and Engineering Effects of the December 29, 2020, M6.4 Petrinja, Croatia Earthquake, and Associated Seismic Sequence, GEER Association Report No. GEER-070, 2021, 10.4154/gc.2021.08

[17] Pollak, D., Gulam, V., Novosel, T., Avanić, R., Tomljenović, B., Hećej, N., Terzić, J., Stipčević, J., Bačić, M., Kurečić, T., Dolić, M., Bostjančić, I., Wacha, L., Kosović, I., Budić, M., Vukovski, M., Belić, N., Špelić, M., Brčić, V., Barbača, J., Kordić, B., Palenik, D., Filjak, R., Frangen, T., Pavić, M., Urumović, K., Sečanj, M., Matoš, B., Govorčin, M., Kovačević, M.S. i Librić, L.: The preliminary inventory of coseismic ground failures related to December 2020 – January 2021 Petrinja earthquake series, Geologia Croatica, 74 (2021), 2, pp. 189–208, https://doi.org/10.4154/gc.2021.08.

[18] Tondi, R.E., Blumetti, A.M., Čičak, M. et al.: 'Conjugate' coseismic surface faulting related with the 29 December 2020, Mw 6.4, Petrinja earthquake (Sisak-Moslavina, Croatia). Sci Rep 11, 9150 (2021). https://doi.org/10.1038/s41598-021-88378-2

[19] Baize, S., Amoroso, S., Belić, N., Benedetti, L., Boncio, P., Budić, M., Cinti, F. R., Henriquet, M., Jamšek Rupnik, P., Kordić, B., Markušić, S., Minarelli, L., Pantosti, D., Pucci, S., Špelić, M., Testa, A., Valkaniotis, S., Vukovski, M., Atanackov, J., Barbača, J., Bavec, M., Brajković, R., Brčić, V., Caciagli, M., Celarc, B., Civico, R., De Martini, P. M., Filjak, R., Iezzi, F., Kurečić, T., Métois, M., Nappi, R., Novak, A., Novak, M., Pace, B., Palenik, D., Ricci, T.: Environmental effects and seismogenic source characterization of the December 2020 earthquake sequence near Petrinja, Croatia, Geophysical Journal International, 230 (2022), 2, pp. 1394-1418, https://doi.org/10.1093/gji/ggac123

[20] Ambraseys, N.N., Jackson, J.A.: Faulting associated with historical and recent earthquakes in the Eastern Mediterranean region, Geophys. J. Int., 133 (1998), pp. 390–406, https://doi.org/10.1046/j.1365-246X.1998.00508.x

[21] Galli, P.: New empirical relationships between magnitude and distance for liquefaction, Tectonophysics, 324 (2000), pp. 169–187, https://doi.org/10.1016/S0040-1951(00)00118-9

[22] Maurer, B.W., Green, R.A., Cubrinovski, M., Bradley, B.A.: Assessment of CPT-based methods for liquefaction evaluation in a liquefaction potential index framework, Geotechnique, 65 (2015), pp. 328–336, https://doi.org/10.1680/geot.SIP.15.P.007

[23] Amoroso, S., Fontana, D., Valvano, C., Wacha, L., Belić, N., Budić, M., Cinti, F.R., Civico, R., De Martini, P.M., Kordić, B., et al.: The liquefaction evidences following the 2020 Petrinja earthquake (Pannonian Basin, Croatia): A full database and insights for phenomena comprehension, Earthquake Spectra, 41(3), pp. 2651-2672, https://doi.org/10.1177/87552930251326561

[24] Bačić, M., Kovačević, M.S., Rossi, N., Librić, L.: Assessing the soil liquefaction susceptibility: a comparative study of CPT and MASW techniques in the aftermath of road failure, in: Proceedings of the 8th International Conference on Road and Rail Infrastructure (CETRA 2024) / Lakušić, S. (ed.), University of Zagreb Faculty of Civil Engineering, Zagreb, 2024, pp. 783-790, https://doi.org/10.5592/CO/CETRA.2024.1540

[25] Bačić, M., Librić, L., Kovačević, M.S.: Liquefaction assessment using a synthetic CPT derived from correlation with shear wave velocity, in: Proceedings of the 3rd Croatian Conference on Earthquake Engineering – 3CroCEE, Split, 19–22 March 2025, pp. 135-145, https://doi.org/10.5592/CO/3CroCEE.2025.148

[26] Bačić, M., Librić, L., Kovačević, M.S.: Comprehensive Multi-Method Assessment of Liquefaction Potential along the levee, in: GeoVadis – Advances in Geotechnical Engineering, CRC Press / Taylor & Francis, pp. 375-380, 2025, https://doi.org/10.1201/9781003645917-57

[27] Amoroso, S., Rollins, K.M., Di Giulio, G., Wacha, L., Urumović, K., Filjak, R., Budić, M., Kordić, B., Palenik, D., Testa, A., Valkaniotis, S., Pucci, S., Benedetti, L., Novosel, T., Bačić, M., Nappi, R.: Geotechnical and geophysical tests following the 2020 earthquake-induced liquefaction phenomena, in: Proceedings of the 2nd Croatian Conference on Earthquake Engineering (2CroCEE 2023), Faculty of Civil Engineering, University of Zagreb, Zagreb, pp. 46-56, https://doi.org/10.5592/CO/2CroCEE.2023.21.

[28] Moiriat, D., Maslac, J., Luong, A.T., Louis, K.J., Kordić, B., et al.: Preliminary results of geotechnical and geophysical investigations on sites with liquefaction occurrences in the greater Petrinja area after the 2020 earthquake, 9th Conference of Croatian Geotechnical Society with International Participation and under the Auspices of ISSMGE, May 2023, Sisak, Croatia, pp. 121–131

[29] Mihaljević, I., Zlatović, S.: Embankments Damaged in the Magnitude Mw 6.4 Petrinja Earthquake and Remediation, Geosciences, 2023, 13(2):48. https://doi.org/10.3390/geosciences13020048

[30] Mihaljević, I., Rupčić, B., Kaić, M., Grget, G., Matešić, L.: Design and construction for rehabilitation of earthquake-damaged water protection levees – methodology and solutions, in: Proceedings of the 4th European Regional Conference of IAEG (EUROENGEO 2024), IAEG / University of Zagreb Faculty of Civil Engineering, Dubrovnik, pp. 587–594, https://doi.org/10.5592/CO/EUROENGEO.2024.245

[31] Seed, H.B., Idriss, I.M.: Simplified procedure for evaluating soil liquefaction potential, Journal of Soil Mechanics and Foundations Division, 97 (1971), SM9, pp. 1249–1273, https://doi.org/10.1061/JSFEAQ.0001662

[32] Boulanger, R., Wilson, D., Idriss, I.: Examination and Re-evaluation of SPT-Based Liquefaction Triggering Case Histories, Journal of Geotechnical and Geoenvironmental Engineering, 138 (2012), 8, pp. 898–909, https://doi.org/10.1061/(ASCE)GT.1943-5606.0000668

[33] Idriss, I., Boulanger, R.: 2nd Ishihara Lecture: SPT- and CPT-based relationships for the residual shear strength of liquefied soils, Soil Dynamics and Earthquake Engineering, 68 (2015), pp. 57–68, https://doi.org/10.1016/j.soildyn.2014.09.010

[34] HRN EN 1998-1:2011: Design of structures for earthquake resistance - Part 1: General rules, seismic actions and rules for buildings, Hrvatski Zavod za Norme, 2011.

[35] HRN EN 1998-1:2011/NA:2011/A1:2021 Eurocode 8: Design of structures for earthquake resistance – Part 1: General rules, seismic actions and rules for buildings – National Annex, Hrvatski Zavod za Norme, 2011.

[36] USGS: M6.4–2 km WSW of Petrinja, Croatia, ShakeMap, URL:https://earthquake.usgs.gov/earthquakes/eventpage/us6000d3zh/shakemap/intensity (accessed 8 October 8th 2025)

[37] Wald, D.J., Quitoriano, V., Heaton, T.H., Kanamori, H.: Relationships between Peak Ground Acceleration, Peak Ground Velocity, and Modified Mercalli Intensity in California, Earthquake Spectra, 15 (1999), 3, pp. 557-564, https://doi.org/10.1193/1.1586058

[38] Atkinson, G.M., Kaka, S.I.: Relationships between felt intensity and instrumental ground motion in the Central United States and California, Bulletin of the Seismological Society of America, 97 (2007), 2, pp. 497–510, https://doi.org/10.1785/0120060154

[39] Caprio, M., Tarigan, B., Worden, C.B., Wiemer, S., Wald, D.J.: Ground motion to intensity conversion equations (GMICEs): A global relationship and evaluation of regional dependency, Bulletin of the Seismological Society of America, 105 (2015), 3, pp. 1476–1490, https://doi.org/10.1785/0120140286

[40] Atkinson, G.M., Wald, D.J.: "Did You Feel It?" Intensity Data: A Surprisingly Good Measure of Earthquake Ground Motion, Seismological Research Letters, 78 (2007), 3, pp. 362–368, https://doi.org/10.1785/gssrl.78.3.362

[41] Bozorgnia Y., Abrahamson N.A., Atik L.A., et al. NGA-West2 Research Project, Earthquake Spectra, 2014;30(3), pp. 973-987. https://doi.org/10.1193/072113EQS209M

[42] Douglas, J.: Earthquake ground motion estimation using strong-motion records: a review of equations for the estimation of peak ground acceleration and response spectral ordinates, Earth-Science Reviews, 61 (2003), 1-2, pp. 43–104, https://doi.org/10.1016/S0012-8252(02)00112-5.

[43] Abrahamson, N.A., Silva, W.J., Kamai, R.: Summary of the ASK14 ground-motion relation for active crustal regions, Earthquake Spectra, 30 (2014), 3, pp. 1025-1055, https://doi.org/10.1193/070913EQS198M

[44] Boore, D.M., Stewart, J.P., Seyhan, E., Atkinson, G.M.: NGA-West2 equations for predicting PGA, PGV, and 5 %-damped PSA for shallow crustal earthquakes, Earthquake Spectra, 30 (2014), 3, pp. 1057-1085, https://doi.org/10.1193/070113EQS184M

[45] Campbell, K.W., Bozorgnia, Y.: NGA-West2 ground motion model for the average horizontal components of PGA, PGV, and 5 %-damped linear acceleration response spectra, Earthquake Spectra, 30 (2014), 3, pp. 1087-1115, https://doi.org/10.1193/062913EQS175M

[46] Chiou, B.S.J., Youngs, R.R.: Update of the Chiou and Youngs NGA model for the average horizontal component of peak ground motion and response spectra, Earthquake Spectra, 30 (2014), 3, pp. 1117-1153, https://doi.org/10.1193/072813EQS219M

[47] Zhao, J.X., Zhou, S., Zhou, J., Zhao, C., Zhang, H., Zhang, Y., Gao, P., Lan, X., Rhoades, D. A., Fukushima, Y., Somerville, P.G., Irikura, K.: Ground-motion prediction equations for shallow crustal and upper-mantle earthquakes in Japan using site class and simple geometric attenuation functions, Bulletin of the Seismological Society of America, 106 (2016), 4, pp. 1552–1569, https://doi.org/10.1785/0120150063.

[48] Akkar, S., Sandıkkaya, M.A., Bommer, J.J.: Empirical ground-motion models for point- and extended-source crustal earthquake scenarios in Europe and the Middle East, Bulletin of Earthquake Engineering, 12 (2014), pp. 359–387, https://doi.org/10.1007/s10518-013-9461-4

[49] Cauzzi, C., Faccioli, E., Vanini, M., Bianchini, A.: Updated predictive equations for broadband (0.01–10 s) horizontal response spectra and peak ground motions, based on a global dataset of digital acceleration records, Bulletin of Earthquake Engineering, 13 (2015), pp. 1587–1612, https://doi.org/10.1007/s10518-014-9685-y

[50] USGS, V_{s30} Models and Data—Earthquake Hazards Program, URL: https://earthquake.usgs.gov/data/vs30/ (accessed September 7th 2025)

[51] Stanko, D., Markušić, S.: Site amplification model for Croatia estimated by random vibration theory-based site response analysis. Soil Dynamics and Earthquake Engineering, 179 (2024), 108547. https://doi.org/10.1016/j.soildyn.2024.108547

[52] Markušić, S., Stanko, D., Penava, D., Ivančić, I., Bjelotomić Oršulić, O., Korbar, T., Sarhosis, V.: Destructive M6.2 Petrinja Earthquake (Croatia) in 2020 - Preliminary Multidisciplinary Research. Remote Sens. 13 (2021), 1095. https://doi.org/10.3390/rs13061095

[53] Herak, M., Markušić, S., Ivančić, I.: Attenuation of Peak Horizontal and Vertical Acceleration in the Dinarides Area. Studia Geophys. Geod. 45 (2001), pp. 383–394.

[54] Markušić, S., Herak, M., Herak, D., Ivančić, I.: Peak Horizontal-to-Vertical Acceleration Ratio and Local Amplification of Strong Ground Motion. Studia Geophys. Geod. 46 (2002), pp. 83–92.

[55] HRN EN 1998-5:2011 Eurocode 8: Design of structures for earthquake resistance: Foundations, retaining structures and geotechnical aspects, Hrvatski Zavod za Norme, 2011.

[56] Seed, H.B., Idriss, I.M., Arango, I.: Evaluation of liquefaction potential using field performance data, Journal of Geotechnical Engineering, 109 (1983), 3, pp. 458–482, https://doi.org/10.1061/(ASCE)0733-9410(1983)109:3(458)

[57] Seed, H.B., Tokimatsu, K., Harder, L.F., Chung, R.M.: Influence of SPT procedures in soil liquefaction resistance evaluations, Journal of Geotechnical Engineering, 111 (1985), 12, pp. 1425-1445, https://doi.org/10.1061/(ASCE)0733-9410(1985)111:12(1425)

[58] Youd, T.L., Idriss, I.M.: Liquefaction resistance of soils: Summary report from the 1996 NCEER and 1998 NCEER/NSF workshops on evaluation of liquefaction resistance of soils, Journal of Geotechnical and Geoenvironmental Engineering, 127 (2001), 10, pp. 817–833, https://doi.org/10.1061/(ASCE)1090-0241(2001)127:10(817)

[59] Boulanger, R.W., Idriss, I.M.: CPT and SPT based liquefaction triggering procedures, Rep. No. UCD/CGM-14/01, University of California, Davis, California, 2014., 138 pp.

[60] Moss, R.E.S., Seed, R.B., Olsen, R.S.: Normalizing the CPT for overburden stress, Journal of Geotechnical and Geoenvironmental Engineering, 132 (2006), 3, pp. 378–387, https://doi.org/10.1061/(ASCE)1090-0241(2006)132:3(378)

[61] Robertson, P.K.: Discussion of 'CPT-based probabilistic soil characterization and classification' by K. Onder Cetin and Cem Ozan, Journal of Geotechnical and Geoenvironmental Engineering, 135 (2009), 1, pp. 84–107, https://doi.org/10.1061/(ASCE)GT.1943-5606.0000120

[62] Andrus, R.D., Stokoe, K.H.: Liquefaction resistance of soils from shear-wave velocity, Journal of Geotechnical and Geoenvironmental Engineering, ASCE, 126 (2000), 11, pp. 1015–1025, https://doi.org/10.1061/(ASCE)1090-0241(2000)126:11(1015)

[63] Robertson, P.K.: Interpretation of cone penetration tests — a unified approach, Canadian Geotechnical Journal, 46 (2009), 11, pp. 1337–1355, https://doi.org/10.1139/T09-065

[64] Kovačević, M.S., Gavin, K., Reale, C., Librić, L., Jurić Kaćunić, D.: Developing correlations between the soil fines content and CPT results using neural networks, in: Sigursteinsson, H., Erlingsson, S., Bessason, B. (Eds.), Proceedings of the XVII ECSMGE-2019, Reykjavik: Icelandic Geotechnical Society, 2019, pp. 1-8, https://doi.org/10.32075/17ECSMGE-2019-0244

[65] Bačić, M., Andačić, K., Gavin, K., Urumović, K.: Soil investigations as a cornerstone for geotechnical design of liquefaction mitigation measures below levees, in: Proceedings of the 4th European Regional Conference of IAEG (EUROENGEO 2024), University of Zagreb Faculty of Civil Engineering, Zagreb, 2024, pp. 218-227, https://doi.org/10.5592/CO/EUROENGEO.2024.257

[66] Grget, G., Matešić, L., Pećina, I., Šindler, D., Šuto, I.: Sanacija temelja Mosta Gromova u Sisku, 9th Conference of Croatian Geotechnical Society with International Participation and under the Auspices of ISSMGE, May 2023, Sisak, Croatia

[67] Bago, M., Matešić, L., Mlinarić, I.: Osvrt na pregled spremnika sirove nafte terminala Sisak nakon potresa 2020. godine, 9th Conference of Croatian Geotechnical Societ with International Participation and under the Auspices of ISSMGE, May 2023, Sisak, Croatia

[68] American Association of State Highway and Transportation Officials (AASHTO): Guide Specifications for LRFD Seismic Bridge Design, AASHTO, 2009, 258

[69] ISSMGE (International Society for Soil Mechanics and Geotechnical Engineering): Manual for zonation on seismic geotechnical hazards. The Japanese Geotechnical Study, International Society for Soil Mechanics and Geotechnical Engineering, 209 p,. 1999.

[70] URL: https://leveeliq.eu/ (accessed October 28th 2025)

[71] GDDA (General Directorate of Disaster Affairs): Seismic Microzonation for Municipalities – Manual, Republic of Turkey, Ministry of Public Works and Settlement, General Directorate of Disaster Affairs, 137 p,. 2004.

[72] SM Working Group: Guidelines for Seismic Microzonation, Conference of Regions and Autonomous Provinces of Italy – Civil Protection Department, Rome, 2015.

[73] California Geological Survey: Special Publication 117A: Guidelines for Evaluating and Mitigating Seismic Hazards in California, California Department of Conservation, 2012.

[74] New Zealand Geotechnical Society: Earthquake geotechnical engineering practice - Module 3: Identification, assessment and mitigation of liquefaction hazards, New Zealand Geotechnical Society, 2016.

[75] Lai, C.G., Conca, D., Famà, A., Özcebe, A.G., Zuccolo, E., Bozzoni, F., Meisina, C., Bonì, R., Poggi, V., Cosentini, R.M.: Mapping the liquefaction hazard at different geographical scales. In Earthquake geotechnical engineering for protection and development of environment and constructions, CRC Press, 14 p., 2019.